To the Graduate Council:

I am submitting herewith a thesis written by Kenneth Ryan Harvey entitled "Behavior and Analysis of Integral Abutments." I have examined the final copy of this thesis for form and content and recommend that it be accepted in partial fulfillment of the requirements for the degree of Master of Science, with a major in Civil Engineering.

Edwin G. Burdette

Dr. Edwin G. Burdette, Major Professor

We have read this thesis and recommend its acceptance:

Accepted for the Council:

Associate Vice Chancellor and
Dean of the Graduate School

BEHAVIOR AND ANALYSIS OF

INTEGRAL ABUTMENTS

A Thesis

Presented for the

Master of Science Degree

The University of Tennessee, Knoxville

Kenneth Ryan Harvey

August 1997

ACKNOWLEDGEMENTS

I am grateful to a number of individuals whose contributions led to the completion of this thesis. I wish to thank my major professor, Dr. Edwin G. Burdette, for his support and guidance. Dr. Burdette has been a source of inspiration to me throughout my graduate and undergraduate studies at The University of Tennessee. I would also like to thank the other members of my committee, Dr. J. Harold Deatherage and Dr. David W. Goodpasture for their assistance during this research project and my academic studies.

Many graduate and undergraduate students have contributed to this research project. Among those I would like to thank are Laura Arico, Jim Bernardi, Oliver Chiang, Chris Myers and Tony Zeind.

I would like to express my appreciation to the Tennessee Department of Transportation. Their quest for new and innovative ideas make this type of research possible.

Lastly, I would like to thank my wife, Jamie, and my family. Their sacrifices, understanding and continual support have made it possible for me to achieve this goal.

ABSTRACT

Integral abutments are used by many states as a standard design for short to medium span bridges. Their widespread use can be attributed to many factors including cost effectiveness, ease of maintainability, and constructability. The Tennessee Department of Transportation (TDOT) is no exception.

The same factors which make integral abutments advantageous for short to medium spans also make them desirable for longer spans. Unfortunately, high stresses, encountered when designing for longer spans, are difficult to justify using current design specifications because of the lack of knowledge regarding the pile-abutment interface and pile soil interaction. This lack of knowledge led to field research currently being conducted by The University of Tennessee, Knoxville under contract with the Tennessee Department of Transportation.

The integral abutment field research consists of an integral abutment which is cast atop a single steel H-pile. The integral abutment will be subjected to slowly applied lateral loads to achieve deflections typical of those experienced by thermal expansion. A total of six tests will be performed, three with a target deflection of ½" and three with a target deflection of 1".

Results from the test are not yet available but preliminary analysis of the abutment indicates that the concrete in the abutment will fail before a ½" deflection is reached. Observation will confirm, first, whether the prediction is correct and , second, whether

the failure will be catastrophic or if the abutment will be capable of further deflection without losing its structural integrity.

TABLE OF CONTENTS

LIST OF FIGURES

CHAPTER 1

INTRODUCTION

Integral bridge abutments have been widely used in the United States for almost sixty years. While they are effective in reducing construction and maintenance costs, limitations in design have confined their use to short and medium span bridges. Designers have long relied on experimentation and experience in integral bridge abutments because of their limited knowledge of pile-soil interaction and the interaction of the pile with the abutment cap (1). In April 1996, a research project, funded by the Tennessee Department of Transportation (TDOT), was initiated by The University of Tennessee to obtain data describing pile-soil and pile-cap behavior both to document existing design approaches and to develop more effective design methodology (2).

1.2 HISTORICAL DEVELOPMENT

Examples of integral bridge abutments may be traced back to the early history of the world, yet integral bridge abutments as they exist today originated around the 1920's. The Ohio Department of Highways, under the direction of J.R. Burkey, began using continuous construction for multiple span bridges during this time. These bridges, known as an "open spandrel rib arch" design, consisted of concrete decks continuous between piers with expansion joints at piers and abutments. These slab designs were developed because of concerns about the use of intermediate concrete expansion joints in the construction of bridge decks. Evolution of this design eventually led to the elimination of expansion joints at the piers leaving only the joints at the abutments (3).

During the 1930's, Ohio bridge designers continued in their quest to eliminate expansion joints by using the same concepts which were used in their arch designs. It was also during this time period that a new method became available to aid their design. At this time designers used simple spans to design multiple span bridges. In 1930, Hardy Cross published a paper entitled "Analysis of Continuous Frames by Distributing Fixed-End Moments" in the Proceedings of the American Society of Civil Engineers. The method described in Cross's paper, now commonly referred to as "moment distribution", helped to pave the way for the elimination of expansion joints and the first bridge design using integral bridge abutments (4).

With the advent of the integral abutment, many other details were designed to advance their use, such as field butt welding of steel members and better support foundations including friction and end-bearing piles (3). The use of integral bridge abutments became widespread as other states began to use this type of design for short to moderate bridge lengths. Eventually, experience in the design and construction of integral abutment bridges led to their use in longer spans as well. A recent study in 1991 indicated that 11 states are currently designing and constructing integral bridges which span up to 300 ft. Two states, Missouri and Tennessee, are designing spans up to 600 and 800 ft. respectively. Currently, the Tennessee Department of Transportation (TDOT) uses integral bridge abutments as a standard design (4).

1.3 ANALYSIS AND DESIGN

Since the introduction of integral abutments, few advances in design have emerged. This lack of advance is due to the difficulty of gaining information about the interaction of the soil and the pile. For this reason, engineers have typically relied more on experience and observation than on conventional design procedure. Recent technological advances are beginning to allow engineers to use mathematical relationships to design integral bridge abutments more accurately through the use of computer analysis. The design approach of the Tennessee Department of Transportation revolves around the use of computer analysis. The TDOT design relies on the computer analysis program, "COM624P- Laterally Loaded Pile Analysis Program For The Microcomputer", to obtain pile response.

There are several reasons why the analysis of a laterally-loaded pile cannot be performed using the typical equations of static equilibrium. The deflection of the pile is solely dependent upon the soil response, and inversely the soil response is dependent upon the amount of deflection. For this reason the analysis must be performed by solving a differential equation to determine the deflection. Since the deflection is different at each point along the length of the pile, the soil response is also dependent on the location along the length of the pile. In order to begin the analysis, a curve of soil response (p) vs. deflection (y), commonly known as the p-y curve, must be determined for points along the pile. The p-y curve is predicted by COM624P using equations based on experimental tests and the in-situ soil properties. Additional information which also must be input is the geometry of the pile and the type of loading that the pile will experience. From the p-y curve a soil modulus (Es), defined as the slope of the p-y curve, can be determined at various points along the pile for various deflections (5).

The basis for the computer analysis of the laterally-loaded pile is the differential equation for the deflection of a beam-column. This equation must be used in order to account for the effects of the axial load as well as the lateral load applied by the integral abutment bridge. This equation has the following general form:

$$\frac{d^2M}{dx^2} + P_x\frac{d^2y}{dx^2} - \frac{dV_v}{dx} = 0 \qquad (1\text{-}1)$$

x - length of pile

y - lateral deflection of pile

P_x - axial load

V_v - shearing force = $\dfrac{dy}{dx} \cdot EI$

M - moment at pile section = $\dfrac{d^2y}{dx^2} \cdot EI$

After the appropriate substitutions, this equation culminates in a fourth order differential equation with the first order term being the product of the soil modulus (E_s) times the deflection of the pile (y). From this group of generated p-y curves, the equations are iterated until the appropriate solution is obtained. Once the analysis is complete, plots of the deflection and moment vs. depth may be retrieved as part of the data (5).

With the TDOT approach, in order to begin the integral abutment design, the length of the structure and expected temperature range must be decided upon and the coefficient of thermal expansion determined. While the length and temperature range are constants of the design, the value of the coefficient of expansion to use in the design must be chosen. Typical values of the linear coefficient of thermal expansion range from .000006 to .000012 /°C (0.0000033 to 0.0000067/°F) (6). From this information, the unrestrained expected thermal movement can be calculated (1).

The second step in the design involves two critical aspects of the integral abutment, the plastic moment capacity of the pile and the moment capacity of the pile-abutment interface. The moment capacity of the pile must be large enough to resist the moment induced by the thermal expansion. Likewise the moment capacity of the pile-abutment interface must be enough to ensure that the pile can achieve this induced moment without cracking of the pile cap.

From the COM624P program, the deflection at which plastic rotation of the pile occurs can be determined. This determination is accomplished by modeling the pile assuming a fixed head condition (1). By determining this point, all subsequent analyses using COM624P and calculations which involve thermal expansion beyond this deflection point can be assigned a maximum moment equal to the plastic moment of the pile. The plastic moment capacity of the pile, M_p, can be calculated by the product of the yield stress of the pile (F_y) times the plastic section modulus (Z_x).

In order to determine the moment capacity of the pile-abutment interface it is first necessary to calculate the forces acting at the top and bottom of the length of the pile embedded in concrete, an embedment depth which is typically one foot. These forces are induced over the width of the pile flange by the concrete in bearing. By equating the moment produced by these forces to the plastic moment of the pile, an f'c necessary to develop the plastic moment can be calculated. Research conducted by Burdette, Jones, and Fricke has indicated that concrete bearing capacity in confined concrete can approach 3.78f'c (11). Based on this value an approximate safety factor for developing the plastic moment can be determined (1).

The next step in the design process is the determination of a column interaction diagram for the pile. In order to obtain the interaction diagram, the use of the COM624P program for analysis again becomes necessary. The analysis is performed by modeling the pile in the fixed head condition under the expected thermal expansion. This analysis yields plots of the p-y curves, pile deflections vs. depth, and pile moment vs. depth. From the plot of pile moment vs depth, the unbraced length of the column can be determined as the distance between points of zero moment. The interaction diagram for the pile may then be developed using conventional column design methods. Service loads for the pile are determined and then factored using applicable AASHTO group loadings. Comparison of the expected loads and the interaction diagram then determines the adequacy of the pile.

CHAPTER 2

KEY CONSIDERATIONS IN DESIGN

2.1 INTRODUCTION

While there are many aspects to the design of an integral abutment, there are two key considerations in assuring that the abutment can accommodate the necessary thermal expansion. The first consideration is the design of the pile-abutment interface. The pile-abutment interface must be properly designed to assure that the pile has the opportunity to develop its plastic moment without failure of the abutment. The second consideration is the design of the pile which must have adequate capacity to resist the weight of the abutment while resisting the lateral load applied by thermal expansion.

2.2 PILE-ABUTMENT INTERFACE

The design of the pile-abutment interface is one of the most important elements in the design of the integral abutment. Without the required capacity, the abutment will crack before the plastic moment is achieved in the pile. Because of the importance of this aspect, it is a key step in the design approach of the Tennessee Department of Transportation. In the TDOT approach, the pair of forces generated by the concrete in bearing multiplied by their moment arm is equated to the plastic moment of the pile. This equation enables the calculation of a required f'c of the concrete used in the abutment. A factor of safety is calculated using a bearing capacity in confined concrete of 3.78f'c (1).

The problem of the concrete cracking in the abutment before reaching the plastic moment of the pile was encountered during the initial phases of this research at The

University of Tennessee. The results of this research were reported in an M.S. thesis at The University of Tennessee by Zeind (8). The lab research conducted consisted of two simulated concrete abutments, one unreinforced and one reinforced, each measuring 4 ft x 2.5 feet by 2.67 feet. A four foot section of an HP 10x42 steel pile was embedded one foot deep into the concrete (8).

The first test was performed on the unreinforced simulated abutment. The pile was instrumented with foil strain gages on the inside flanges at 1 inch, 6 inches and 11 inches below the concrete-pile interface. These gages were applied with a special heat-curing epoxy. Foil gages were also installed on the pile above the concrete level at 1 inch, 9 inches, and 17 inches. These foil gages were installed with M-Bond 200 epoxy on the outside flanges of the pile (8).

A hydraulic ram was used to load the pile and was attached to the pile at a height of 27.5 inches above the concrete. During loading, the rotational movement of the simulated abutment was restricted using a steel frame constructed of tube sections. This frame was placed on top of the simulated abutment and bolted to the floor of the laboratory. Tube sections were also placed at the base of the concrete block to resist translation. Through load application by a hydraulic ram, the simulated abutment was tested to failure. At a load of approximately 30 kips, resulting in a moment of 68.8 kip-ft., a tension failure occurred in the concrete block before the plastic moment of the pile of 150 kip-ft. could be achieved (8).

Due to the unexpected failure which occurred in the unreinforced concrete specimen, a second test was conducted using a reinforced concrete block. The reinforcement design was adopted from a typical TDOT integral abutment design and was constructed of #7 and #5 bars. The setup of the second test was essentially the same as the first, with the exception of a few modifications. It was decided that weldable strain gages would be better suited to resist the jarring caused by the impact of the pile driver in the planned field test piles. These gages were not only more durable, they were also much easier to apply which cut down significantly on the time necessary to gage the pile. The second modification was the use of three pressure sensors to measure the pressure associated with the concrete-pile interaction. Two of these sensors were installed on the compression flange of the pile while the third was installed on the tension flange. The block was again restrained against movement using a similar system which was slightly modified to provide further restraint. The simulated abutment was again loaded to failure using the hydraulic ram. Despite the reinforcing steel this test produced similar results to the first test. A tension failure occurred in the concrete at approximately 36 kips before the pile could achieve its plastic moment (8).

The results of these lab tests are inconclusive due to the differences between the simulated tests and an actual integral abutment. Despite apparent differences in the two applications, the results demonstrate that better information about the interaction and behavior of the pile and abutment are needed.

While a solution has not been developed to arrest the problem of cracking abutments when using steel H-piles, if such a problem actually exists, abutment details have recently been developed to eliminate this problem when using concrete piles. Research performed by Kamel, Benak, Tadros, and Jamshidi at the University of

Nebraska-Lincoln has concluded that through the use of a sliding joint for the pile-abutment connection, more thermal expansion could be accommodated than by using a fixed pile-abutment connection. The four sides of the proposed joint are constructed using polystyrene or styrofoam. When this material is used, the bond is broken between the concrete pile and the concrete poured for the abutment on the four faces of the pile. The material is used to accommodate the thermal expansion in the lateral direction. The top of the joint consists of a neoprene bearing pad with a teflon coating applied to the top side. The teflon coating bears against a steel plate which is embedded into the abutment and allows sliding of the pile against the abutment. The joint, which can be manufactured in one piece, fits over the top of the concrete pile. When expansion occurs, the abutment which slides across the pile after a lateral force of approximately 5 kips, can accommodate approximately 1 inch of thermal expansion (9).

2.3 DESIGN OF THE PILE

The design of the pile is also an important factor in the integral abutment design. Accordingly, the design of the pile is a key step in the TDOT design of the integral abutment bridge. The TDOT pile design begins by predicting the deflected shape of the pile. The deflected shape is established using the COM624P microcomputer program by entering key variables which include soil properties, pile geometry, and expected thermal deflection. The thermal expansion is induced at the ground level, and corresponding deflections are shown at various depths for the given variables. After determining the deflection vs. depth, the unbraced length of the pile is determined from the plot of the pile moment vs. depth. These pile moments result from the expected thermal deflection which was input into COM624P. The unbraced length used in the design equations is taken as the distance between the two points of zero moment located on the moment vs. depth curve. An interaction diagram for the pile is then developed using capacity equations for combined axial load and bending which are taken from the AASHTO Standard Specifications for Highway Bridges (10).

$$\frac{P}{0.85A_sF_{cr}}+\frac{MC}{M_u\left(1-\frac{P}{A_sF_e}\right)}\leq 1.0 \tag{2-1}$$

$$\frac{P}{0.85A_sF_y}+\frac{M}{M_p}\leq 1.0 \tag{2-2}$$

Where:

$$F_{cr}=F_y\left[1-\frac{F_y}{4\pi^2\mathrm{E}}\left(\frac{KL_c}{r}\right)^2\right] \quad \text{for} \quad \frac{KL_c}{r}\leq\sqrt{\frac{2\pi^2\mathrm{E}}{F_y}} \tag{2-3}$$

$$F_{cr}=\frac{\pi^2\mathrm{E}}{\left(\frac{KL_c}{r}\right)^2} \quad \text{for} \quad \frac{KL_c}{r}>\sqrt{\frac{2\pi^2\mathrm{E}}{F_y}} \tag{2-4}$$

$$C=0.6+0.4a\geq 0.4 \tag{2-5}$$

K - effective length factor taken as 0.875

L_c - length of member between points of zero moment (in) r - pile radius of gyration in the plane of buckling (in)

F_{cr} - buckling stress (psi)

C - equivalent moment factor used when the ends of the beam column are restrained against sidesway

M - Allowable moment in pile.

P - Allowable axial load in pile.

E - Modulus of elasticity of steel = 29,000,000 psi

F_y - Yield stress of steel

C may be taken as 1 conservatively. In the above equation, *a* is the ratio of the smaller to larger end moment which is positive when moments act opposite to each other and negative when they act in the same direction.

M_u = maximum flexual strength of the pile cross-section

M_p = plastic moment of the pile cross-section

$$F_e = \frac{E\pi^2}{\left(\frac{KL_c}{r}\right)^2} \qquad (2\text{-}6)$$

F_e - Euler Buckling stress in the plane of bending

The interaction diagram takes account of the fact that the pile is experiencing both axial force from the abutment and bending from the thermal expansion. After the development of the interaction diagram, the factored loads for various conditions are compared to determine if the column has adequate strength.

CHAPTER 3

FIELD TESTING TO OBTAIN INFORMATION

3.1 INTRODUCTION

In December 1996, preparation began for the first of four field tests under the abutment research contract. The planned field test will be a continuation of the lab testing performed at The University of Tennessee during the initial phases of the abutment research project. The purpose of this field testing is to obtain better information concerning the pile-abutment interface and the forces acting on the pile by more accurately modeling the abutment and instrumenting the embedded pile.

3.2 SITE DESCRIPTION

Field testing is being conducted in Knoxville, Tennessee. The pile was driven on a construction site which will later become a part of the Dutchtown Road interchange on Pellissippi Parkway. The pile in the first test was located in an area of undisturbed soil which can be classified as a stiff clay. The 40 ft. pile was driven to a depth of approximately 38 ft., leaving 2 ft. exposed, one foot for instrumentation and one foot to insert into the abutment.

3.3 TEST SETUP

Several additions to the site were necessary in order to begin the field test. Two reaction pads , 4 ft. by 4 ft. , were constructed on the site to support the abutment beam.

In an attempt to minimize the effects of the reaction pad on the pile and to minimize the length of the abutment beam which would be needed, the reaction pads were located 14 ft. apart, and the center of the supporting beam is 6.7 ft. from the center of the pile. An 8 ft. by 8 ft. concrete pad was constructed approximately 23 ft. from the pile to support the frame from which a horizontal load will be applied to the abutment. The abutment was then constructed, and ballast blocks were cast on top of it to achieve the desired weight (Fig. 1)*.

3.4 DESIGN OF TEST ABUTMENT

Several important design properties of the test abutment were considered to accurately model an actual abutment and thus increase the reliability of the information obtained in the tests. The key properties considered were the stiffness of the test abutment, the reinforcement used in the test abutment, and the measure of the reaction needed to prevent rotation of the abutment.

3.4.1 STIFFNESS OF THE TEST ABUTMENT

In order to develop a moment at the pile-abutment interface similar to that experienced by an actual integral abutment, it is important to have a comparable stiffness. In an actual integral abutment the stiffness is achieved through the use of girders which act compositely with the bridge deck. In the test abutment it was not possible to obtain the stiffness in this manner; therefore, the desired stiffness was achieved by using a

* All figures are located in Appendix A.

combination of the simulated abutment beam/deck and a steel member used to support the end of the simulated abutment beam (Fig. 1). In order to determine the desired stiffness of the system, a value for the stiffness of an actual integral abutment was calculated. This value was determined by considering an integral abutment bridge with the following parameters as a model:

- AASHTO/PCI type III prestressed beams spaced at 6 ft. o.c.
- 7" slab with f'c = 5000psi.
- 90 foot span.

This model was chosen because it was typical of the components and properties used in an actual integral abutment bridge. The value of the stiffness for this model, k_θ, was calculated to be 260,335 k-ft/rad.

The next step in the calculation was to determine the amount of stiffness provided by the abutment beam, assuming the beam is simply supported over 6.54 ft. by the steel support beam and the pile. The stiffness, k_s, represents the stiffness of the steel beam used to support the simulated abutment beam. The stiffness of the abutment beam, k_θ, is first calculated assuming the steel support beam has infinite stiffness, $k_s = \infty$ as follows:

$$I = \frac{b \cdot h^3}{12} = \frac{(72) \cdot (30)^3}{12} = 162{,}000\, in^4 \tag{3-1}$$

If E is approximated as 4,031 ksi, the follow calculation can be performed:

$$k_\theta = \frac{3EI}{L} = \frac{3(4{,}031)(162{,}000)(1/144)}{6.54} = 2{,}080{,}218\ {kip - ft}\!\!\left/_{rad}\right. \tag{3-2}$$

This value is equivalent to 8.0 times the stiffness of the typical integral abutment bridge and therefore requires additional flexibility. This flexibility can be achieved by using a support beam with the appropriate stiffness k_s. The stiffness can be calculated by first determining the angle θ which results from a deflection Δ (inches) of the abutment beam at the steel support beam:

$$\theta^{RAD.} = \frac{\Delta}{6.54' \cdot 12\ in/ft} = 0.0127\ \Delta \tag{3-3}$$

$$M = 6.54' \times 12\, in/ft \times R \tag{3-4}$$

$$R = k_s \cdot \Delta \tag{3-5}$$

$$M = (78.5) \cdot k_s \cdot \Delta$$

From these expressions the equivalent rotational stiffness can be calculated:

$$\text{Equivalent Rotational Stiffness}\,(k_\theta) = \frac{M}{\theta} = 6{,}181 k_s \tag{3-6}$$

A W18 x 106 shape was chosen for the beam to add the necessary flexibility to the system. The stiffness of the member was calculated in the following manner:

$$k_s = \frac{48EI}{L^3} = \frac{48 \cdot 29{,}000\ ksi \cdot 1910\ in^4}{(192\ in)^3} = 375.64\ k/in \tag{3-7}$$

From the stiffness of the beam, k_s, it is possible to calculate the equivalent rotational stiffness k_θ of the beam and the equivalent stiffness of the system k_{EQ}:

$$k_\theta = (6{,}181)(k_s) = {(6{,}181)(375.64)}/{12} = 193{,}486\ kip - ft / rad$$

$$\frac{1}{k_{EQ}} = \frac{1}{k_{\theta(Abutment\ Beam)}} + \frac{1}{k_{\theta(Support\ Beam)}} = \frac{1}{2{,}080{,}218} + \frac{1}{193{,}486} \qquad (3\text{-}8)$$

$$k_{EQ} = \frac{1}{5.65x10^{-6}} = 177{,}021\ k - ft/rad$$

As can be seen from the preceding calculations the stiffness of the system is greatly dependent on the stiffness of the support beam. While the test abutment turned out to be less stiff than the "typical" integral abutment bridge considered, it was not practical to stiffen the system beyond the value just determined.

3.4.2 ABUTMENT REINFORCEMENT

In order to ensure that the test abutment was representative of a typical integral abutment, it was reinforced in the same manner as those designed by the Tennessee Department of Transportation (TDOT). The reinforcement details were taken directly from TDOT design drawings and consisted of a 2'-2" by 2'-8" rectangular cage made of # 5 bent bars. To this cage was added # 7 bars which run longitudinally the width of the abutment (Fig. 2).

The primary objective in the reinforcement of the abutment beam was to resist the moment generated by the reaction at the support beam. The abutment beam was designed by equating the maximum moment to the cracking moment and solving for the required depth of the beam. Since the beam depth is calculated in this manner, the amount of steel required is equal to the minimum amount as prescribed by ACI 318-95, which came out to be approximately 6.00 in^2. The reinforcement chosen consisted of 12 # 7 bars, six in the top portion and six in the bottom, running the length of the abutment beam. To facilitate placement, four 22" by 5'-6" rectangular cages made of # 5 bent bars were spaced equally the length of the abutment beam (Fig. 3).

3.4.3 REACTION MEASUREMENT

As mentioned previously, a major concern in modeling the integral abutment was to have a test system with a stiffness as close as possible to an actual abutment. The abutment beam support was an important element in developing this stiffness. While this support aided in developing the stiffness, it made the measurement of the pile moment more difficult. To determine this moment, it is necessary to measure the reaction at the abutment beam support. By measuring this reaction, the moment can be determined from the free body diagram of the abutment and the equations of statics. Summation of the moments at the centerline of the pile yields the following equations:

$$\sum M_A = 3.145V - 6.54R + M_{PILE} = 0 \qquad (3\text{-}9)$$

Where:

R - reaction at the support beam

V - horizontal load applied to the abutment

$$M_{PILE} = 6.54R - 3.145V$$

The measurement of this reaction is accomplished by inserting a load cell between the abutment beam and the W 18x 106 support beam. The size of the load cell required was calculated by substituting the plastic moment for the value of the pile M_{PILE} and substituting values for the applied load V. Substituting an expected maximum value of V equal to 90 kips yields a value of R equal to 66 kips. Based on this analysis, a 100 kip load cell was chosen for the reaction measurement.

3.5 LOADING REGIMEN

The loading regimen chosen for the field test was an important aspect in correctly modeling the behavior of an actual abutment. In a typical bridge, the thermal expansion begins slowly and gradually increases as the temperature rises. The thermal expansion levels off as the temperature reaches the high point of the day and then begins to decrease consistent with decreases in the temperature. This type of cycle occurs during a typical day with some variation. This loading cycle was used to develop the loading regimen for the simulated abutment.

The loading regimen consists of two parts with three tests in each, for a total of six tests. In order to allow the soil time to remold and to subject the test abutment to a loading typical of that found in an integral abutment bridge, it was decided that only one test would be performed per day. In the first three tests the target deflection is ½ inch and is achieved in four equal steps. Each step is completed in approximately 10 minutes and then held for the remainder of the hour. The final step is completed in approximately 10 minutes, after which the deflection is taken slowly back to zero (Fig 4). The second three tests follow the same pattern as the first tests and have a target deflection of 1". The target deflection is achieved in seven equal steps (Fig 5).

3.6 LOADING SYSTEM

The main component of the loading system for the abutment is the load frame depicted in figure 1. This load frame was developed by the Civil Engineering Department at The University of Tennessee for analyzing free vibrations of bridge piers. The abutment is loaded above the centroid of the pile with the application point being at the center of the abutment beam approximately 4.5 ft. from the ground surface.

It was important to design the connection of the load frame not only to allow ease of connectability but also to allow the abutment to be loaded in two directions. The load frame is connected to the abutment using 1 inch Dywidag post-tensioning steel threadbars. These bars have an ultimate strength of 127.5 kips and are manufactured by Dywidag Systems International (12). To accomplish the connection of the Dywidag bars to the concrete abutment beam, a 3 inch i.d. steel pipe 14' in length was inserted into the abutment beam form before casting the concrete. The Dywidag bar is then inserted through the pipe and secured against the back side of the abutment beam with a 1 inch steel plate and a threaded nut. A hydraulic jack is placed on the Dywidag bar behind the tube section on the load frame in series with a 100 kip interface load cell. The hydraulic jack is then secured with a 1 inch steel plate and a threaded nut which allows for the application the load using a hydraulic hand pump. The load cell is monitored during the testing using the megadac data acquisition system.

3.7 INSTRUMENTATION

Instrumentation of the pile and abutment was a crucial step in obtaining reliable data. In order to begin the instrumentation, the pile was sandblasted to remove the rust and scale. While not entirely necessary, this made the pile easier to instrument and kept the process cleaner. After the pile was sandblasted, a hand grinder was used to further condition small areas where strain gages would be installed. It was determined that the weldable strain gages would be applied every 18 inches beginning at the ground surface and terminating at 19.5 ft. below the top of the pile. The weldable gages were applied on each flange of the pile to cancel out any effects of torsion. To more easily protect the gages, they were installed on the inside face of the pile flange. After the gages were installed, the wires were marked according to the flange they were on, A, B, C or D, and the depth they were located, beginning with 1 at the top and ending with 14.

The next step in the instrumentation process was the installation of the pressure sensors. It was determined that pressure sensors would be installed on each face of the pile. These pressure sensors were installed at 18 inches o.c. in a staggered pattern to better bound the point of zero lateral pressure. The sensors on face A-B began at 5'-3" from the ground surface and terminated at 12'-9", while sensors on face C-D began at 6'-9" from the ground surface and terminated at 14'-3". These pressure sensors were specially made by the Sensotec Corporation for this project. The sensors measured 2.25 inches across the face and were 2 inches deep. The sensors came drilled and tapped in three locations on the back to facilitate mounting.

It was determined that the easiest way to protect the sensors from damage while driving was to install them directly in the center of the pile face. In order to install them in this location, a hole was first cut in the face of the pile. After cutting the first hole, a slot was cut out directly below it in the web to a depth of approximately 2.5 inches. Because of possible heat damage to weldable gages already installed and the need for a relatively precise cut, a plasma cutter was used to remove the material for the sensors. Tabs were used to mount the pressure sensors to the pile. The tabs were fabricated with a hole in one end which was used to bolt the tab to the back of the pressure sensor. The face of the sensor was aligned flush with the face of the pile and the other end of the tab was welded to the pile. RTV-108 sealant was used to cushion the space between the pile and the pressure sensor. Mounting the sensor in this way was important to minimize the amount of bending that was detected by the pressure sensor.

The final step in the instrumentation process was to protect the instruments from weather damage and damage which could occur while driving the pile. Wires from all gages were first taped into the fillet of the flange and web of the pile. A rubber undercoating was then applied by brush to the wires and gages as an extra precaution to protect the gages from water damage. The next step was the fabrication of sheet metal to protect the instruments from damage during driving. This shielding would protect not only the strain gages but also the back of the pressure sensors. The shielding was fabricated of 18 gage sheet metal which was bent along the edges to facilitate attachment to the pile. This shielding was installed at an angle between the flange and the web of the pile and was then spot welded approximately every foot (Fig. 6). Wedges were fabricated from ¼ inch steel plate and welded to the driving end of the pile at the termination of the shielding. An expandable foam was then applied through predrilled holes in the shielding for added weather protection and to act as a cushion while driving the pile.

Final instrumentation for the test included an embeddable concrete gage. This gage was placed in the abutment form prior to the concrete pour. The location of this gage was based on the lab tests described. The failure of the test specimen in the lab test was observed to propagate at 45° angles to the pile flanges which were in tension. For this reason the gage was placed near the bottom of the abutment on a 45° angle from the pile tension flange.

CHAPTER 4

EXPECTED RESULTS

4.1 INTRODUCTION

Test results are necessary to determine the true behavior of the first integral abutment test specimen. Unfortunately, test results were not available at the time this thesis was written. While all components of the abutment were complete, extreme caution was taken to ensure that the concrete used in the abutment had achieved its full strength. Analysis of the test abutment using the methods presented demonstrates that the extra time will be justified.

4.2 COM624P ANALYSIS OF TEST ABUTMENT

The COM624P program is a vital key to predicting the results of the test. From this program it is possible to obtain expected moments and deflections of the pile due to the load applied to the abutment. To begin the analysis on the test abutment, information regarding the pile geometry, the properties of the soil, and the type of loading were necessary.

The variables for the pile geometry were taken directly from the abutment test with three exceptions. The COM624P program contains a pile library which must be used when analyzing a steel H-pile. By picking the pile size, an HP 10x42, the values contained in the library are inserted for diameter of pile, moment of inertia and the area of the pile.

These values varied only slightly from the typical values found in the AISC Steel Design Handbook.

Variables of pile geometry:

- distance from top of pile to ground surface : 24"
- length of pile : 480"
- pile modulus : 29,000,000 psi
- slope of ground surface : 0°
- diameter of pile : 10.035"
- moment of inertia : 211 in^4
- area of pile : 12.4 in^2

The soil at the test site was classified as a very stiff soil. Several methods were used in an attempt to determine the soil properties needed for the analysis. These methods included using suggested values and attempting to bound the properties using test data obtained from a pilot test performed earlier in the research. The attempts to determine the soil properties using these methods led to answers which were questionable at best. This uncertainty was due in part to the fact that most representative values are dependent on the average undrained shear strength, c. Values of c for a stiff clay given in the COM624P manual have a wide range from 6.94 psi to approximately 28 psi. To determine the correct undrained shear strength, it was necessary to perform tests on soil samples collected from the site. The soil samples were collected from two locations on the site at a depth of approximately 5 pile diameters and within a 10 ft. radius of the pile (Fig. 7).

An unconsolidated undrained triaxial test was performed on the two samples, and a value for the average undrained shear strength, *c* (psi), was obtained. Data and calculations from these tests are included as Appendix B. The value of c obtained was approximately 35 psi which was higher than the highest value given in the COM624P manual. The strain corresponding to one-half the maximum principal stress difference, $\varepsilon 50$, was also determined from the triaxial test. Representative values for the other properties were chosen from the COM624P manual.

Variables of soil properties:

- soil type : very stiff clay above water table
- depth of soil layers : one continuous layer 480"
- soil modulus, k : 2000 pci
- unit weight, γ : .069 pci
- average undrained shear strength, c : 35.24 psi
- internal friction angle, ϕ : 0°
- strain which corresponds to one-half the maximum principal stress difference, $\varepsilon 50$: 0.003

The COM624P program provides great flexibility in loading conditions by allowing the user to model the pile in a free head, fixed head, or partially fixed head, condition or by specifying a deflection and moment. The analysis performed for the test abutment required that the pile be modeled first as a fixed head condition. For the fixed head condition the following parameters must be input:

- shear, (lbs)
- axial load, (lbs)
- slope of the top of the pile, (degrees)

By analyzing the pile as a fixed head condition, the deflection at which the plastic moment of the pile occurs can be obtained. To obtain these results, it was necessary to use trial and error to determine the specific values of interest. The axial load on the pile was set at 65,000 lbs, which was the weight of the test abutment including the ballast. The slope at the top of the pile was set at 0°. By changing the amount of shear, the plastic moment could eventually be achieved. Using this method gave the following values:

Deflection at Mp (in)	Shear required (kips)	Moment (kip-ft)
0.35	47	145

The output files for this analysis are included as Appendix C.

Once the plastic moment of the pile is achieved, the moment remains constant while increased shear will bring about increased deflection. To determine the extra shear required to reach deflections of interest, the COM624P program was again used to analyze the pile. The loading condition used for this analysis specified the deflection and moment. Based on this loading condition, the plastic moment was input in addition to the deflection of interest. The following information resulted:

Deflection of Interest (in)	Base Shear, V (kips)	Additional Shear Required (kips)	Total Shear, V (kips)
1/2	47	3.3	50.3
1	47	10.9	57.9

The output files are also included as Appendix C.

4.3 ANALYSIS USING TDOT DESIGN METHOD

The next step in the prediction of results is the determination of the required f'c of the concrete used in the abutment for the deflections of interest. The Tennessee Department of Transportation accomplishes this using the following methodology:

- Equation of the forces generated by the concrete in bearing

$$Ft = Fb = 0.85fc'(a)(b) \tag{4-1}$$

a : depth of stress block = β_1 c = .85(6”) = 5.1”

b : width of pile = 10.035”

$$c: \frac{\text{Embedment depth}}{2} = \frac{12"}{2} = 6"$$

β_1 : reduction factor based on f'c, ACI 318-95 Section 10.2.7.3

$$Ft = Fb = 43.5fc'$$

- Equation of pile moment to the force couple:

$$M_{pile} = F(Z)$$

$$Z: \left[(\text{Embedment depth}) - (a/2)\cdot 2\right] = 6.9"$$

The moments at the desired deflections found from the COM624P analysis exceed the plastic moment of the pile; therefore, the plastic moment is used in place of these calculated moments. The following values result:

Deflection of Interest (in)	fc' required (psi)
1/2	5800
1	5800

The calculations necessary to determine these values are included as Appendix D (1).

In the final step of the TDOT analysis, the f'c required is compared to the actual f'c used in the abutment to determine if the moment in the pile can be developed. This comparison is based on research by Burdette, Jones, and Fricke which suggests bearing capacity in confined concrete approaches 3.78f'c. From this value, an evaluation of the ability to develop the moment is calculated as follows:

$$\frac{required\ \ fc'}{actual\ \ fc'} \leq 3.78$$

When applied to the calculated values for *f'c* using, an *actual f'c* equal to 5000 psi, a ratio of 1.16 results. This would seem to indicate that the abutment is adequate to develop the required deflections.

Examination of the research performed by Burdette, Jones, and Fricke to acquire the bearing capacity in confined concrete leads one to question the validity this analysis. The test specimens described in "Concrete Bearing Capacity around Large Inserts" consisted of 2 ft. thick concrete slabs which were 12 ft. by 12 ft. in size. The smallest edge distance in these specimens measured from the center of the large inserts was 2 ft. 1 ½ in.. In comparison, the edge distance measured from the face of the embedded pile to the edge of the abutment in the direction of loading is 10 ¼ in. over a 10.035 in. flange width. While bearing capacity in the abutment is most certainly larger than f'c alone, the above comparison would indicate that 3.78 is potentially unconservative for design purposes because it's use neglects the potential failure in tension (9).

4.4 ANALYSIS USING PROPOSED METHOD

While the TDOT design method yields believable results, closer examination of the test abutment reveals four key elements in the analysis which should be modified to obtain results which are more consistent with actual test conditions. These differences constitute the primary differences between the TDOT design method and the proposed analysis method.

The first difference in the two methods is in the calculation of the forces induced on the concrete as a result of the embedded pile. The free body diagram of the test abutment can be drawn as shown in Figure 8, Appendix A. In order to satisfy the equations of equilibrium the following equation must be correct:

$$\sum Fx = 0 = V + Ft - Fb \qquad (4\text{-}2)$$

$$Fb = Ft + V$$

In which,

V - Shear force (kips)

Fb - Force applied at the bottom of the embedded portion of the pile as a result of the pile bearing on the concrete (kips)

Ft - Force applied at the top of the embedded portion of the pile as a result of the pile bearing on the concrete (kips)

The TDOT design method equates the top and bottom forces in the embedded concrete to obtain the moment, neglecting the shear force applied to the abutment. In an actual integral abutment, this shear force would be analogous to the force resulting from the thermal expansion.

The second difference in the TDOT method and the proposed method is in the determination of *a (in.)*, the depth of the stress block for the forces *Ft* and *Fb*. In the TDOT method the depth of the stress block is calculated by assuming half of the embedment depth is in tension and half is in compression as a result of the force applied by the pile. This depth, *c (in)*, is then multiplied by β_1 to obtain the depth of the stress block, *a (in)*. In the proposed design method, the depth a is obtained through iteration of the equations of statics and the equation for the rectangular stress block for concrete in the following manner:

1. The shear (V) and moment of the pile (M_{pile}), for a particular deflection, are obtained from COM624P.
2. Assume a distance for x (in.), the distance between the forces F_b and F_t in the embedded portion of the pile (Fig 8).
3. Iterate using the following process.

As stated in chapter 3, the reaction may be obtained from:

$$R = \frac{3.145V - M_{pile}}{6.54} \tag{4-3}$$

The force Fb can then be determined by taking moments about point e (Fig 6).

$$\Sigma \, Me = 0 = -78.5R + \left(25.74 + \frac{12 - x}{2}\right) \cdot V + Fb(x) \tag{4-4}$$

Solve for F_b.

As previously determined, the force Ft can be obtained by summing the horizontal forces:

$$\Sigma \, Fx = 0 = V + Ft - Fb \tag{4-5}$$

Solve for F_t.

The depth of the rectangular stress block a (in.) can then be determined by the following equation and values:

$$Fb = .85f'c \cdot (a) \cdot (b)$$

f'c - Based on laboratory test conducted at the University of Tennessee this value may be conservatively taken as 5000 psi for state class A concrete mix.

b - Based on the abutment laboratory tests as described in chapter 2, this value is taken as 20". This effective width is determined by averaging the widths between the tension cracks at two points as shown in Figure 9.

The distance between the two forces F_b and F_t , *x* (in.), may then be calculated by considering the depth of the stress block, *a* (in.), to be the same for both forces. This results in the distance *x* being equal to the embedment depth minus *a*. From the calculated value for x, it is then possible to reiterate the equations to refine the x value. Complete calculations are included in Appendix D with the resulting values as follows:

Deflection (in.)	Shear, V (kips)	Moment, M_{pile} (kip-ft)	a (in.)
1/2	50.3	145	2.94
1	57.9	145	3.08

While the TDOT method determines the f'c necessary to prevent crushing of the concrete, the abutment may fail due to tension stress in the concrete. This consideration is the third difference between the proposed analysis method and the TDOT method. The tension stress is calculated at section a-a in figure 6 in a way consistent with a typical punching shear calculation as illustrated in Appendix D.

From this analysis, the stress at section a-a may be calculated for the deflections given above. These calculations yield the following results:

Deflection (in.)	Shear, V (kips)	Stress, f (ksi)
1/2	50.3	0.70
1	57.9	0.73

Calculation of the concrete tensile stress at failure allows a comparison with the actual stress. The tensile stress at failure produced by punching shear is typically taken as:

$$f_{allowable} = 4\sqrt{f'c} = 4\sqrt{5000}/1000 = .282\,ksi \tag{4-9}$$

Comparison of the failure stress to the actual stress indicates failure of the abutment before it achieves a ½" deflection. Thus, some of the most important information to be obtained from the field tests is the response of the concrete abutment in the vicinity of the embedded pile.

CHAPTER 5

CONCLUSIONS AND RECOMMENDATIONS

As previously stated, the first phase of the abutment research project involves a regimen of testing on four separate abutments. These tests should yield a massive amount of data, which can then be analyzed to help determine the true behavior of an integral abutment. Even though test data are not yet available, tentative conclusions can be drawn based on the calculations presented herein. These conclusions may then be evaluated as the testing progresses.

The TDOT design method predicts that the abutment is adequate to support the loads generated by the expected thermal expansion. In contrast, the proposed analysis method predicts that the abutment fails before reaching a ½" deflection. Several scenarios are possible depending on which prediction is confirmed by field testing. If the abutment fails, as predicted by the analysis presented herein, this would indicate that evaluating the strength of the abutment based on $f'c$, as in the TDOT design method, is unconservative. This result would also raise the following questions:

- Does a failure mean a catastrophic failure of the abutment ?
- If a failure occurs, can the expected thermal expansion be achieved ?

A failure at a deflection which is higher than predicted may indicate the need to consider performing a different type of analysis on the abutment. Such a result would also indicate that the larger deflection is achieved through additional flexibility in the system beyond that predicted.

The first abutment test may provide answers to many of the questions presented. Thorough inspection of the abutment, especially in the embedment zone of the pile, will determine if tension failure has occurred without catastrophic failure of the abutment. If catastrophic failure has not occurred, further testing will demonstrate the ability of the abutment to achieve the desired deflections. By measuring the deflection at the ground level and at the center of the abutment beam, differences in the deflection at these two points can be observed. Differences in the deflections in these areas will indicate additional deflection which has been achieved through flexibility of the system.

LIST OF REFERENCES

LIST OF REFERENCES

1. Wasserman, Edward P. and Walker, John H., "Integral Abutments for Steel Bridges." Vol. II, Chapter 5, Highway Structures Design Handbook, American Iron and Steel Institute, October 1996.
2. Burdette, Edwin G., "Behavior of Laterally Loaded Piles Supporting Bridge Abutments." Proposal for research (phase 1) submitted to the Tennessee Department of Transportation. 1995.
3. Burke, Martin P. Jr., "The Genesis of Integral Bridges in Ohio." Concrete International, Issue No. 45. 1996.
4. Burke, Martin P. Jr., "Integral Bridges." Transportation Research Record, Issue No. 1275. 1990.
5. Ensoft, Inc., "COM624P-Laterally Loaded Pile Analysis Program for the Microcomputer, Version 2.0." Austin, Texas. June, 1993.
6. Mehta, Kumar P., *Concrete Structure, Properties and Materials*, Prentice-Hall, Inc., Englewood Cliffs, NJ, 1986 (p 88).
7. Burke, Martin P. Jr., "Integral Bridges: Attributes and Limitations." Transportation Research Record, Issue No. 1393. 1993.
8. Zeind, Anthony F., "Development of Field Testing Procedures to Determine the Behavior of Steel Piles Supporting Integral Abutments." Thesis submitted in partial fulfillment for the requirements for the degree of Master of Science. The University of Tennessee, Knoxville, Tennessee. 1995.

9. Kamel, Mounir R., Benak, Joseph V., Tadros, Maher K., and Jamshidi, Mostafa, "Prestressed Concrete Piles in Jointless Bridges." PCI Journal Vol. 41, Issue No. 2. March-April, 1996.

10. American Association of Highway and Transportation Officials, *Standard Specifications for Highway Bridges*, Sixteenth Ed., 1996

11. Burdette, E. G., Jones, W. D., and Fricke, K.E., "Concrete Bearing Capacity Around Large Inserts." In ASCE Journal of Structural Engineering Vol. 109, No. 6, June 1983.

12. Dywidag Systems International, "Dywidag Threadbar Post-Tensioning System." Bolingbrook, Illinois. 1994.

APPENDICES

APPENDIX A

FIGURES

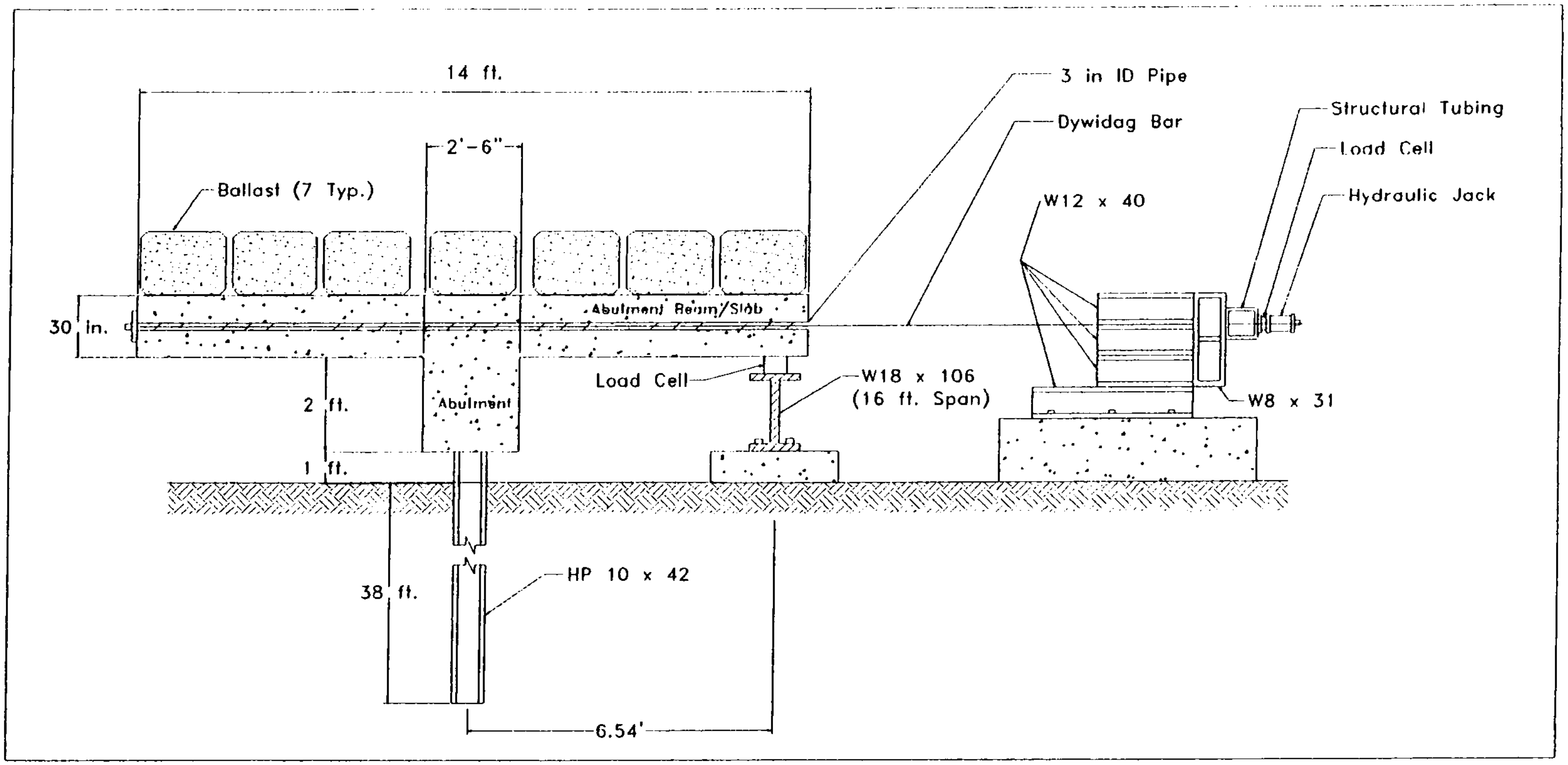

Figure 1: Test setup (not to scale)

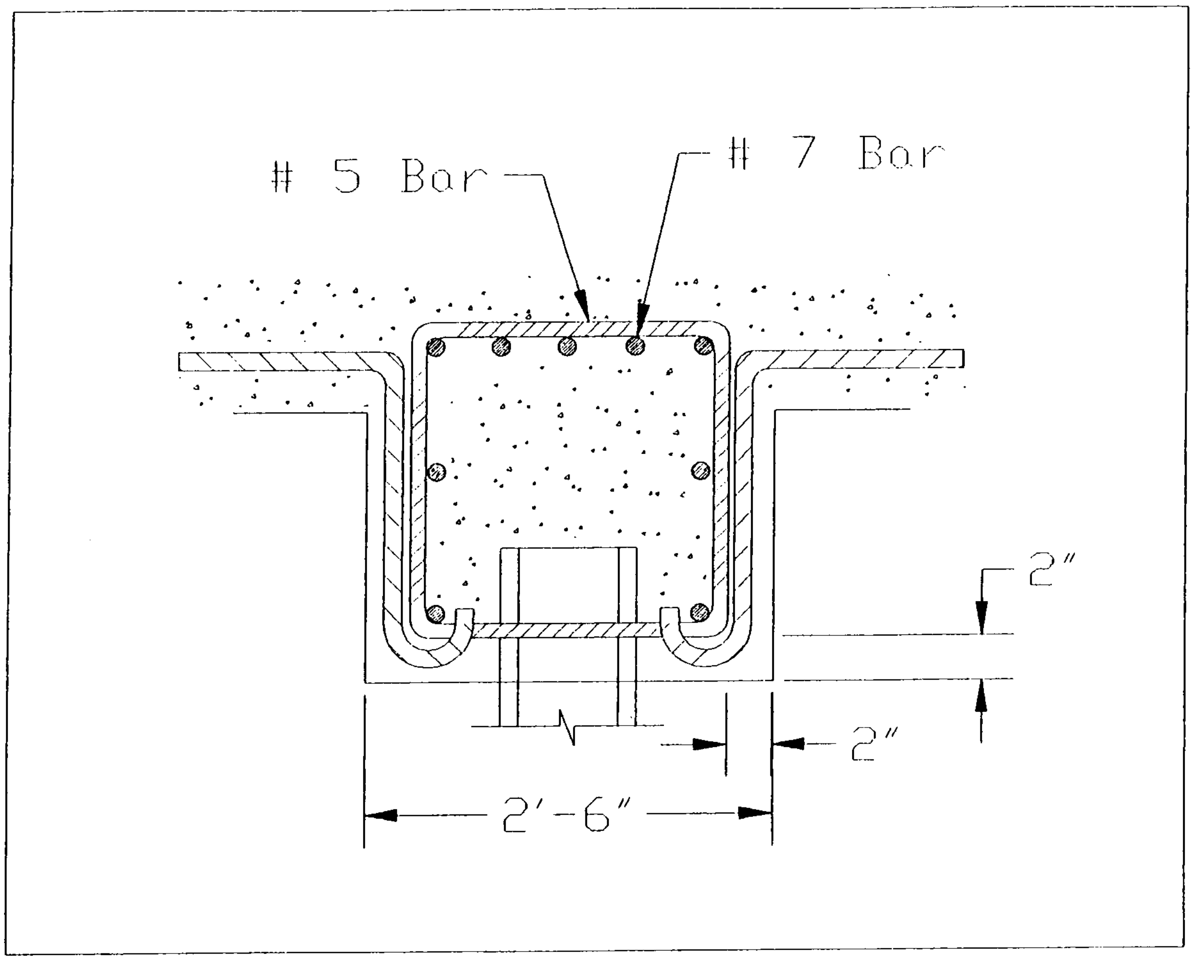

Figure 2: Abutment reinforcement (not to scale)

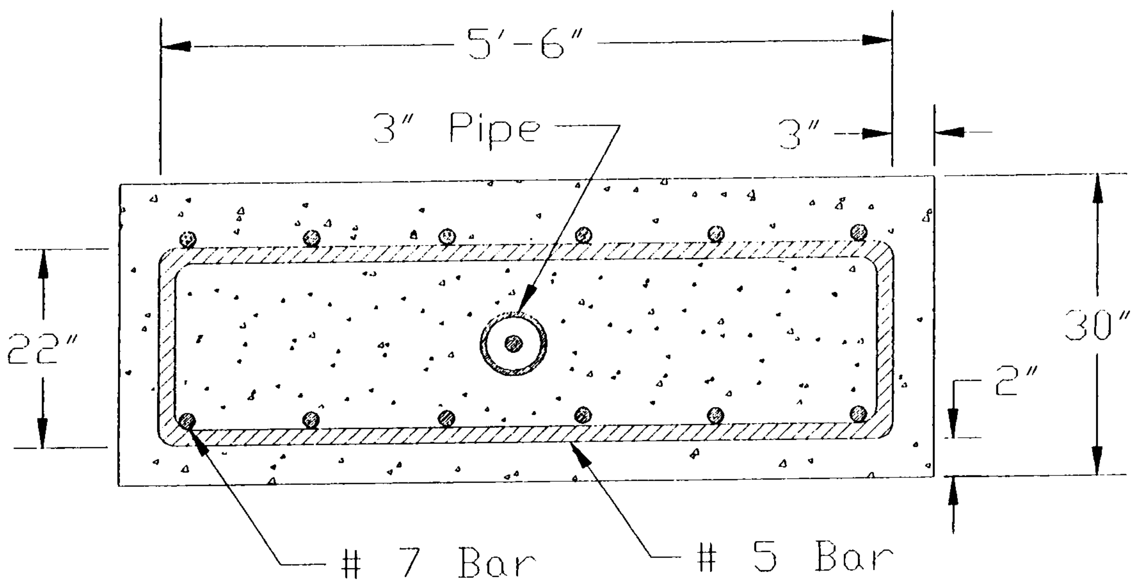

Figure 3: Abutment beam reinforcement (not to scale)

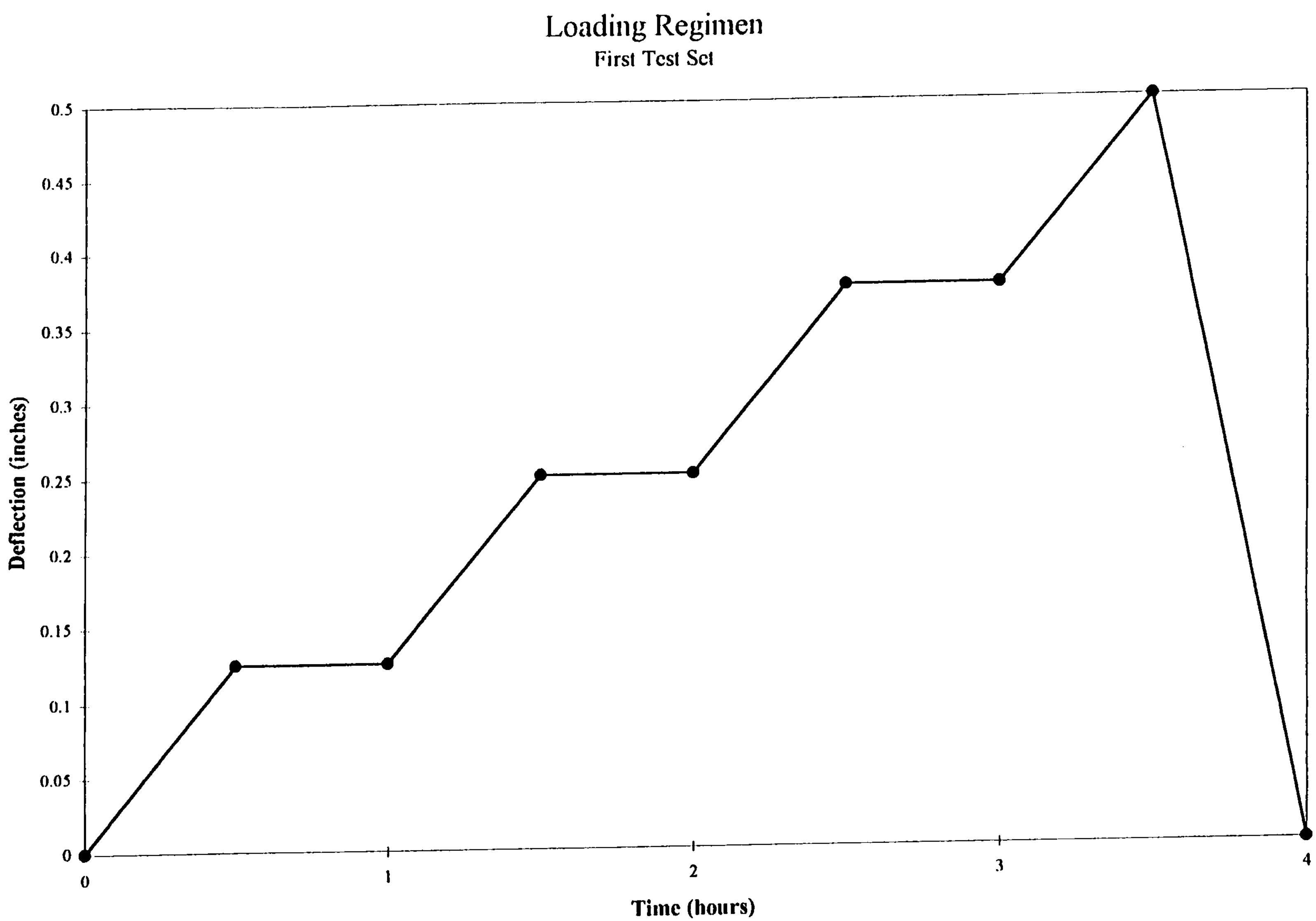

Figure 4: Loading regimen ; First Test Set

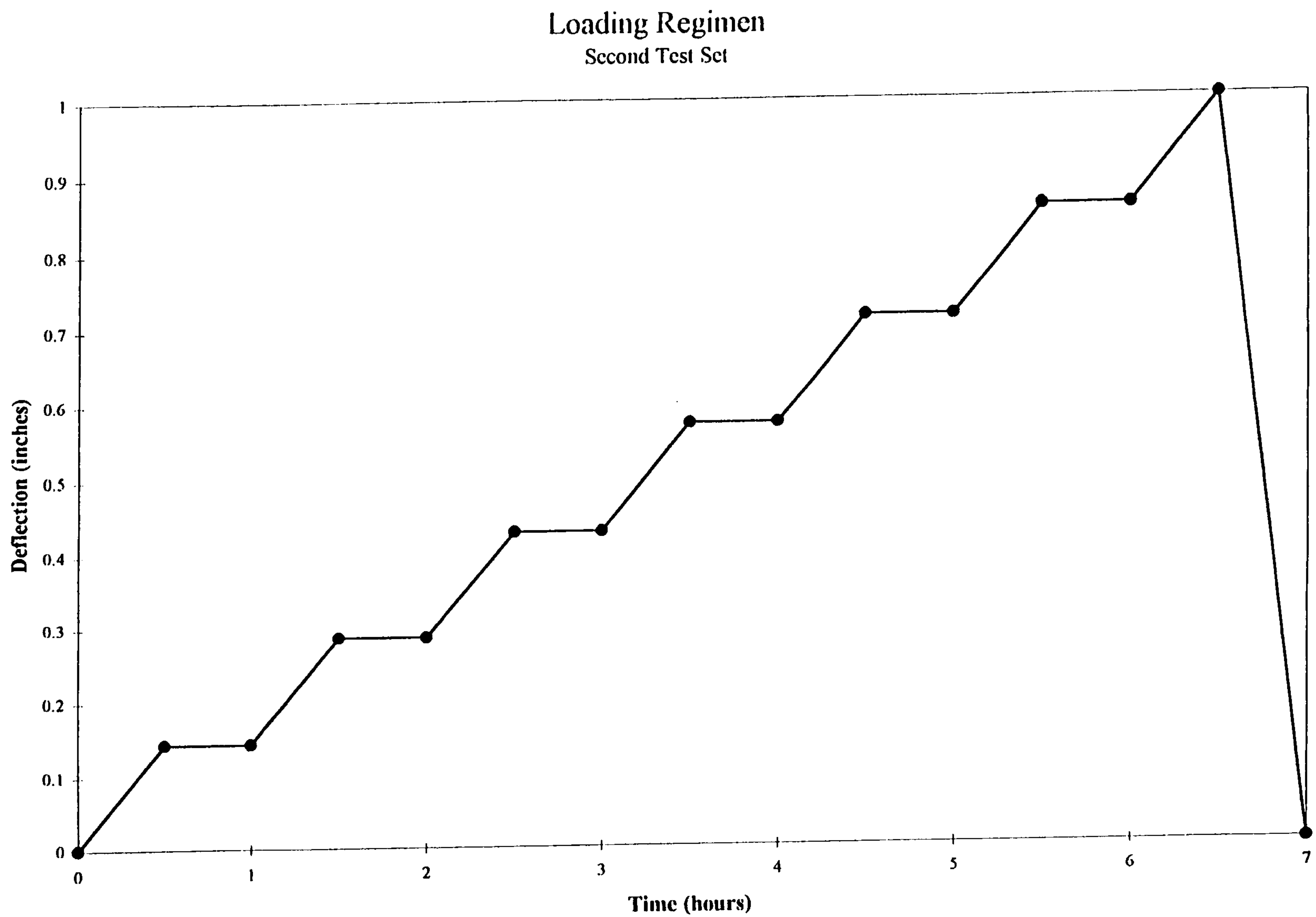

Figure 5: Loading regimen; Second Test Set

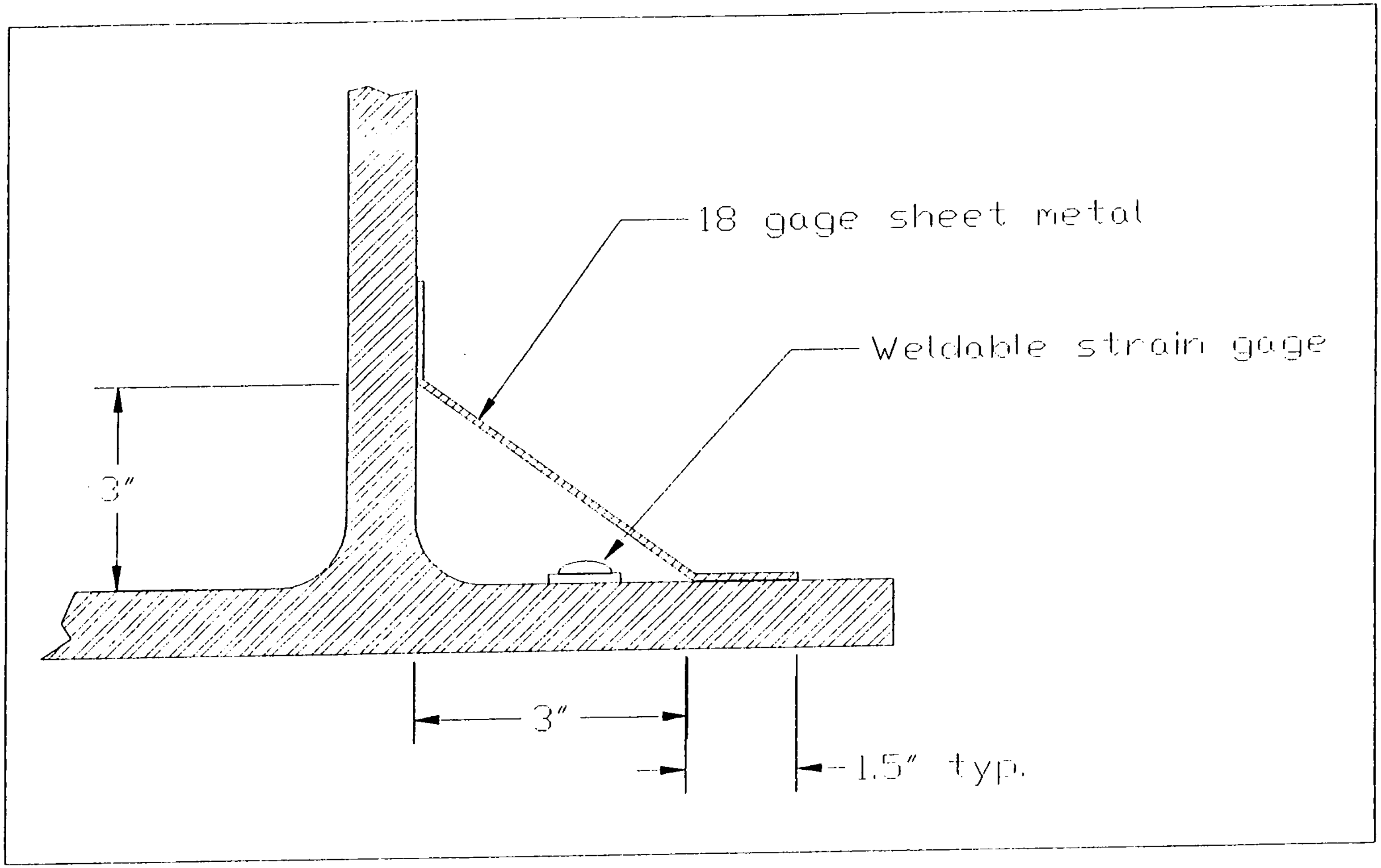

Figure 6: Instrumentation and Shielding (not to scale)

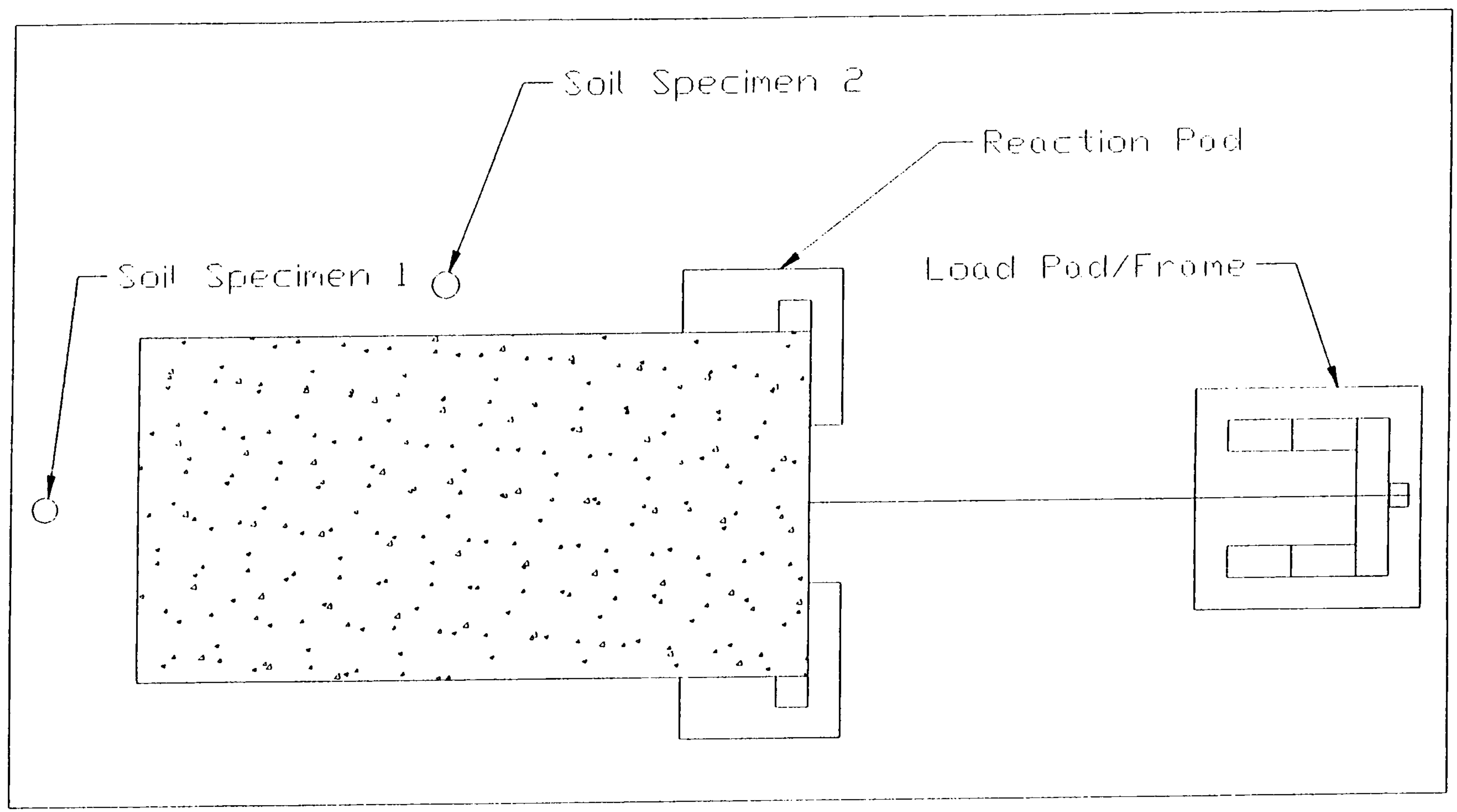

Figure 7: Plan View of Site (not to scale)

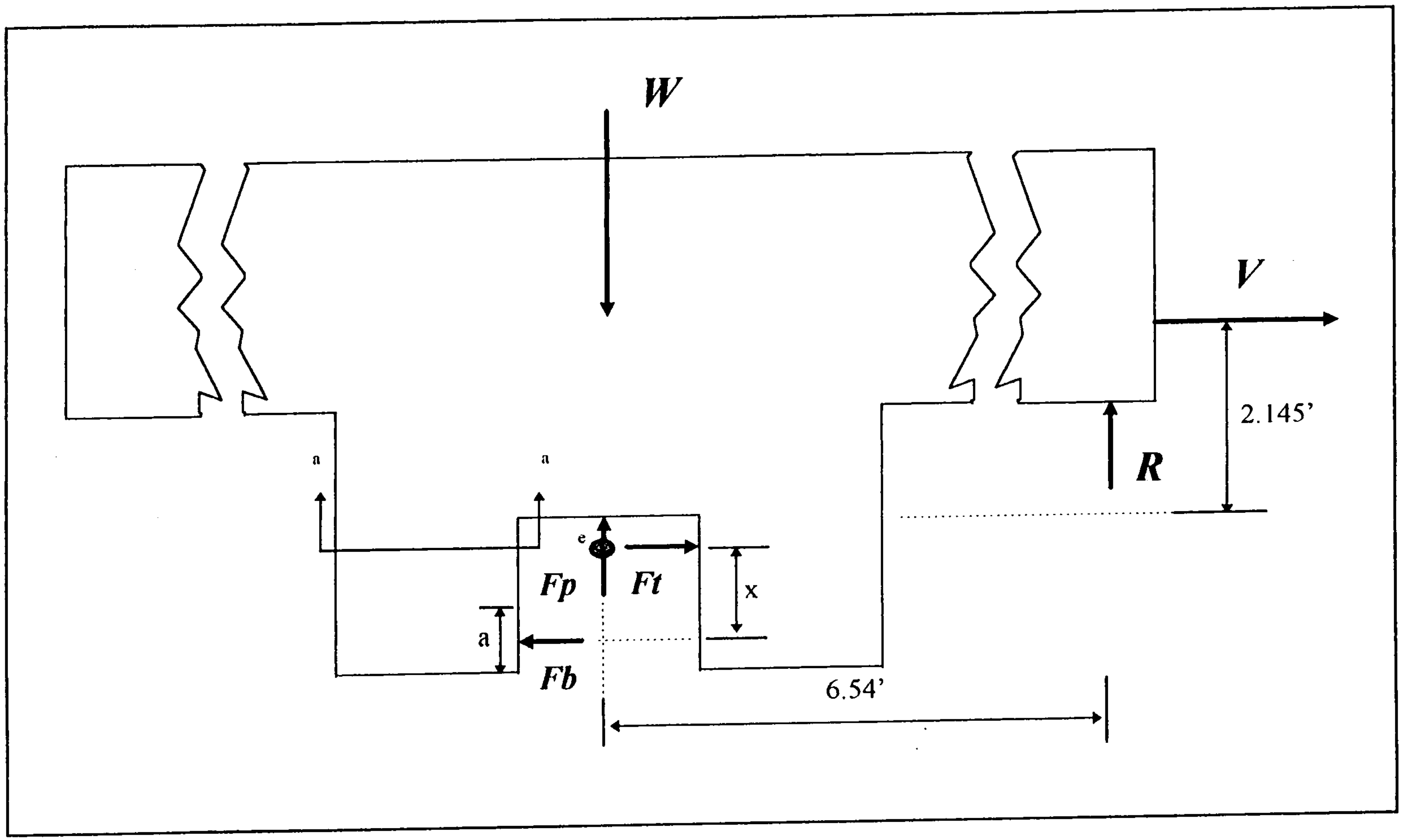

Figure 8: Free Body Diagram of Test Abutment (not to Scale)

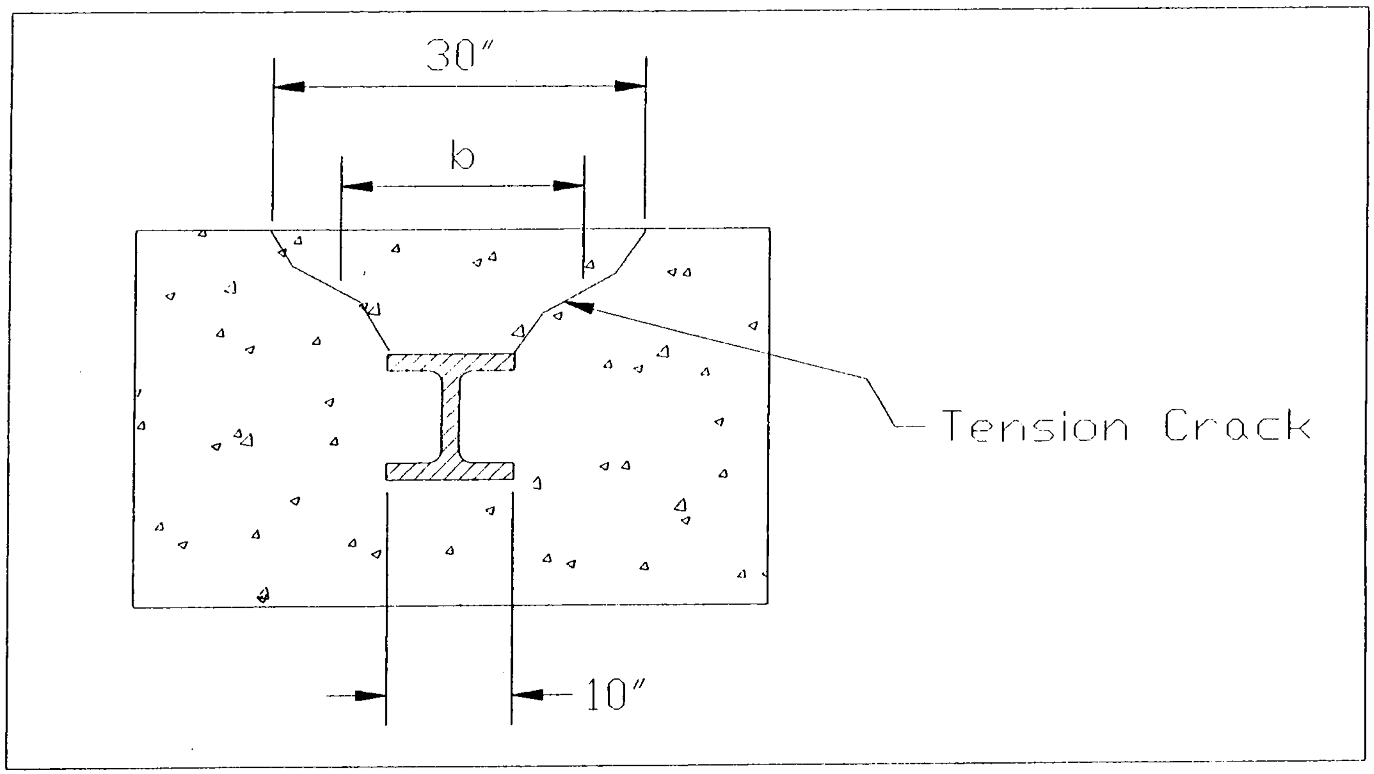

Figure 9: Determination of value for *b* (not to scale)

APPENDIX B

SOIL TEST DATA

University of Tennessee Civil Engineering

Unconsolidated Undrained Triaxial Compression Test

Specimen No. 1

Sample Location Rear of Abutment

Tested by Curtis Allen, Laura Arico, Ken Harvey

Proving Ring Dial Reading	Load lbs.	Strain in.(10^{-4})	Corrected Area in.^{2}	Strain %	Stress psi
11	7.57	20	2.772	0.06	2.72972
27	18.58	40	2.830	0.11	6.56347
50	34.40	60	2.890	0.17	11.9014
71	48.85	80	2.953	0.22	16.5404
90	61.92	100	3.019	0.28	20.5109
112	77.06	120	3.088	0.33	24.9574
132	90.82	140	3.159	0.39	28.7456
147	101.14	160	3.235	0.44	31.2677
158	108.70	180	3.313	0.50	32.8072
163	112.14	200	3.396	0.56	33.0199
162	111.46				
140	96.32				

Method of Calculation:

$$Load = (proving\ ring\ dial\ reading) \cdot .688\ lbs / unit$$

$$Stress = \frac{Load}{Corrected\ Area}$$

$$A_o = \frac{\pi(d^2)}{4} = \frac{\pi(1.86^2)}{4}$$

$$Corrected\ Area = \frac{A_o}{1-\varepsilon}$$

$$\%\ strain = \frac{\varepsilon}{h_o} = \frac{\varepsilon}{3.6}$$

University of Tennessee Civil Engineering

Unconsolidated Undrained Triaxial Compression Test

Specimen No. 2

Sample Location Right of Abutment

Tested by Curtis Allen, Laura Arico, Ken Harvey

Proving Ring Dial Reading	Load lbs.	Strain in.(10^{-4})	Corrected Area in.^{2}	Strain %	Stress psi
14	9.63	20	2.772	0.06	3.47418
35	24.08	40	2.830	0.11	8.50821
65	44.72	60	2.890	0.17	15.4718
91	62.61	80	2.953	0.22	21.1996
115	79.12	100	3.019	0.28	26.2083
132	90.82	120	3.088	0.33	29.4141
148	101.82	140	3.159	0.39	32.2299
161	110.77	160	3.235	0.44	34.2455
175	120.40	180	3.313	0.50	36.3371
185	127.28	200	3.396	0.56	37.4766
183	125.90				
168	115.58				

Method of Calculation:

$$Load = (proving\ ring\ dial\ reading) \cdot .688\ lbs\ /\ unit$$

$$Stress = \frac{Load}{Corrected\ Area}$$

$$Ao = \frac{\pi(d^2)}{4} = \frac{\pi(1.86^2)}{4}$$

$$Corrected\ Area = \frac{Ao}{1-\varepsilon}$$

$$\%\ strain = \frac{\varepsilon}{ho} = \frac{\varepsilon}{3.6}$$

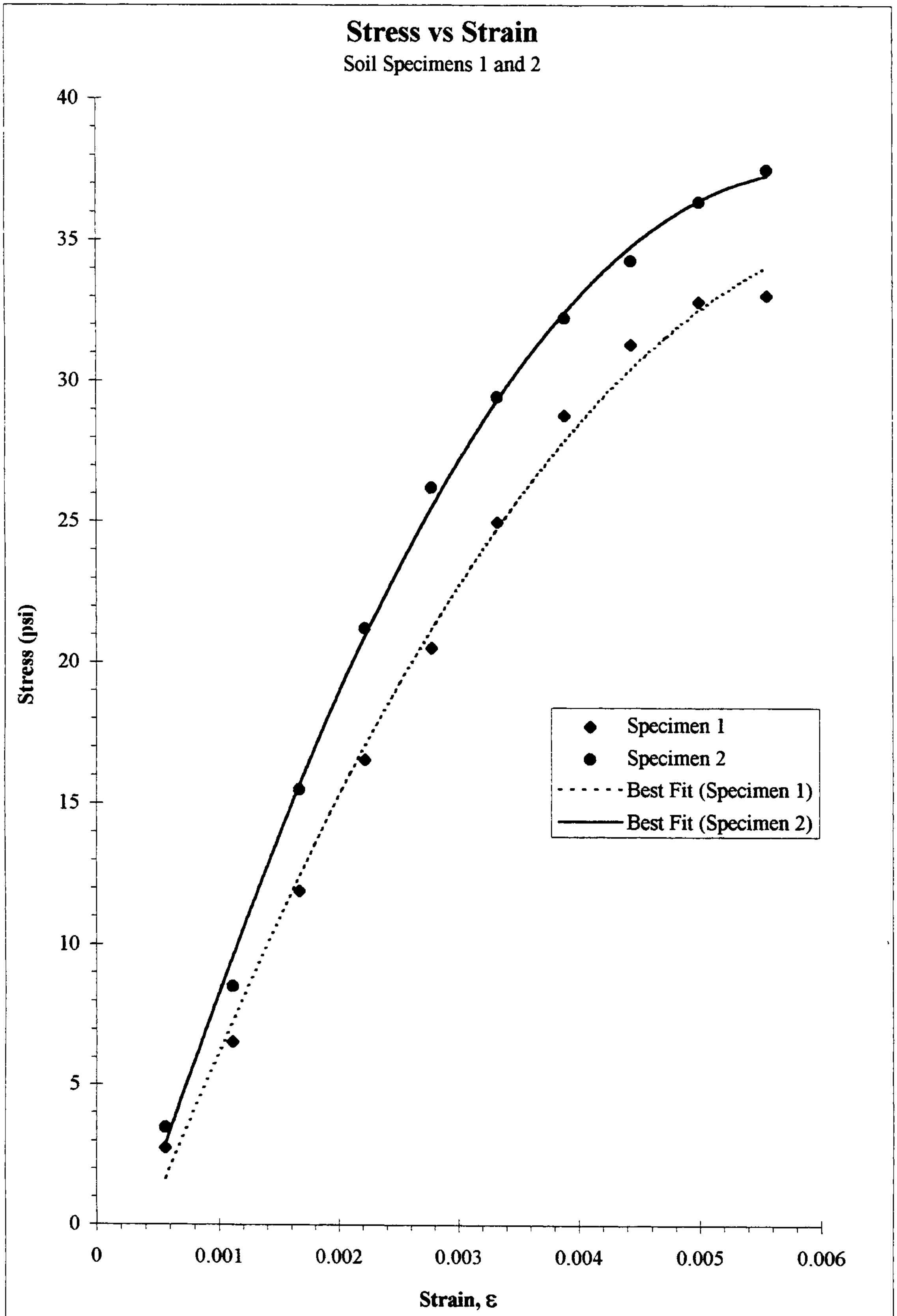

Stress vs Strain
Soil Specimens 1 and 2
Stress (psi)
40
35
30
25
20
15
10
5
0
0
0.001
0.002
0.003
0.004
0.005
0.006
Strain, ε
Specimen 1
Specimen 2
Best Fit (Specimen 1)
Best Fit (Specimen 2)

APPENDIX C

COM624P OUTPUT

Determination of deflection and shear which
produces the plastic moment in the pile.

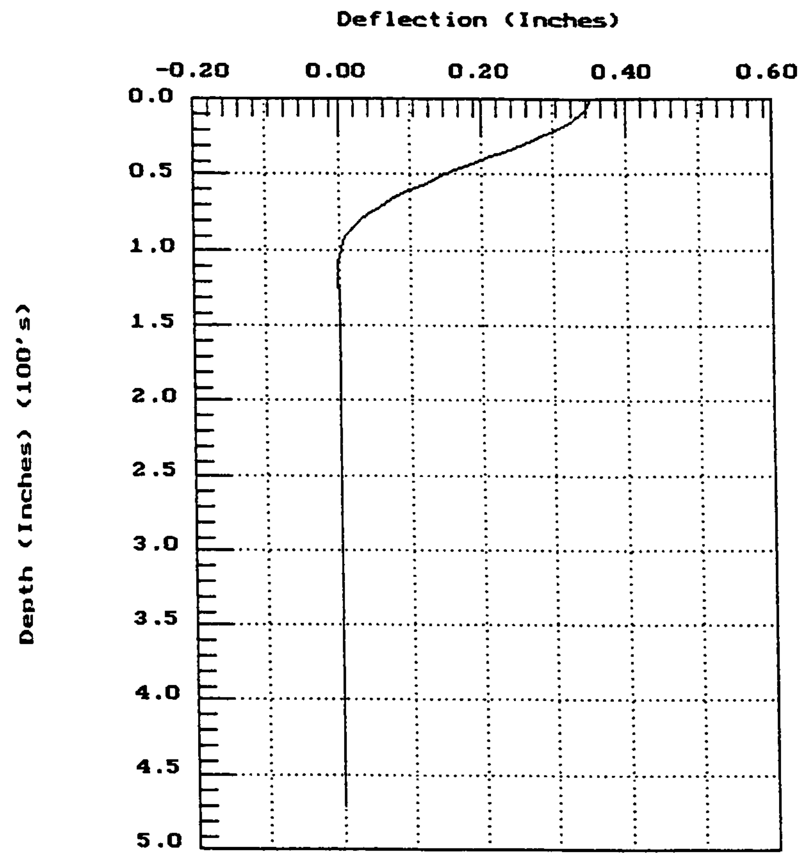
Deflection (Inches)
-0.20
0.00
0.20
0.40
0.60
0.0
0.5
1.0
1.5
2.0
2.5
3.0
3.5
4.0
4.5
5.0
Depth (Inches) (100's)

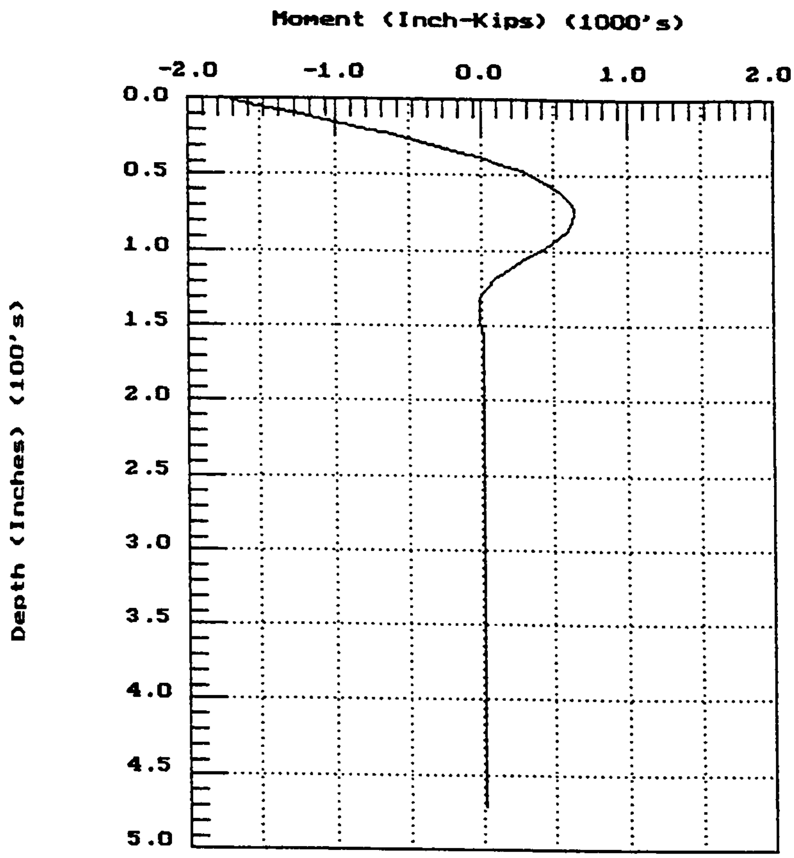
Moment (Inch-Kips) (1000's)
-2.0
-1.0
0.0
1.0
2.0
0.0
0.5
1.0
1.5
2.0
2.5
3.0
3.5
4.0
4.5
5.0
Depth (Inches) (100's)

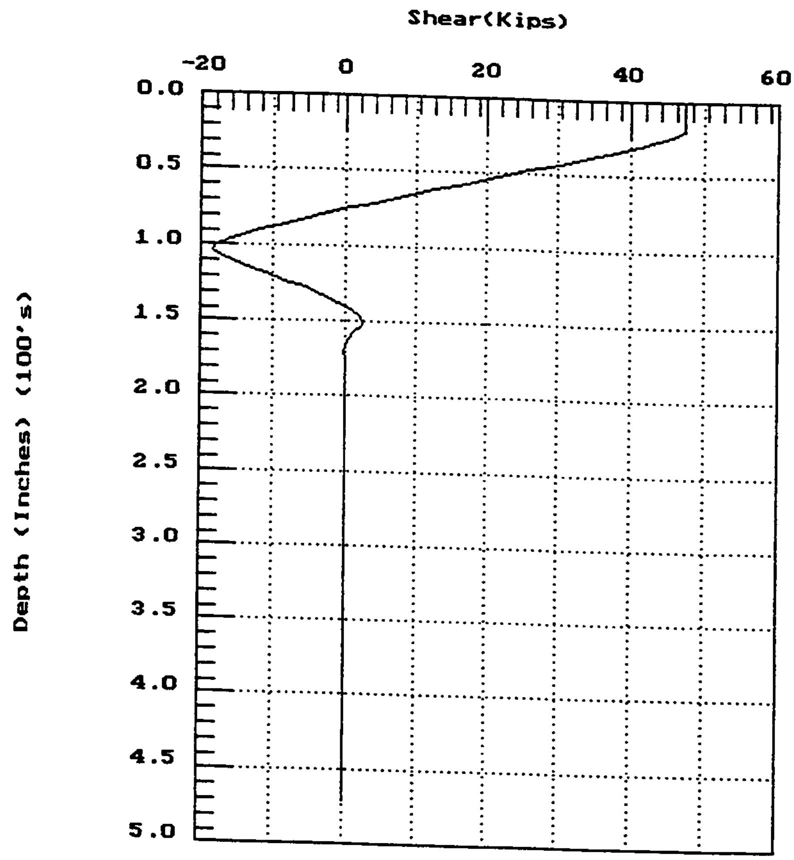

Shear(Kips)
-20
0
20
40
60
0.0
0.5
1.0
1.5
2.0
2.5
3.0
3.5
4.0
4.5
5.0
Depth (Inches) (100's)

Determination of additional shear required to
achieve ½" deflection.

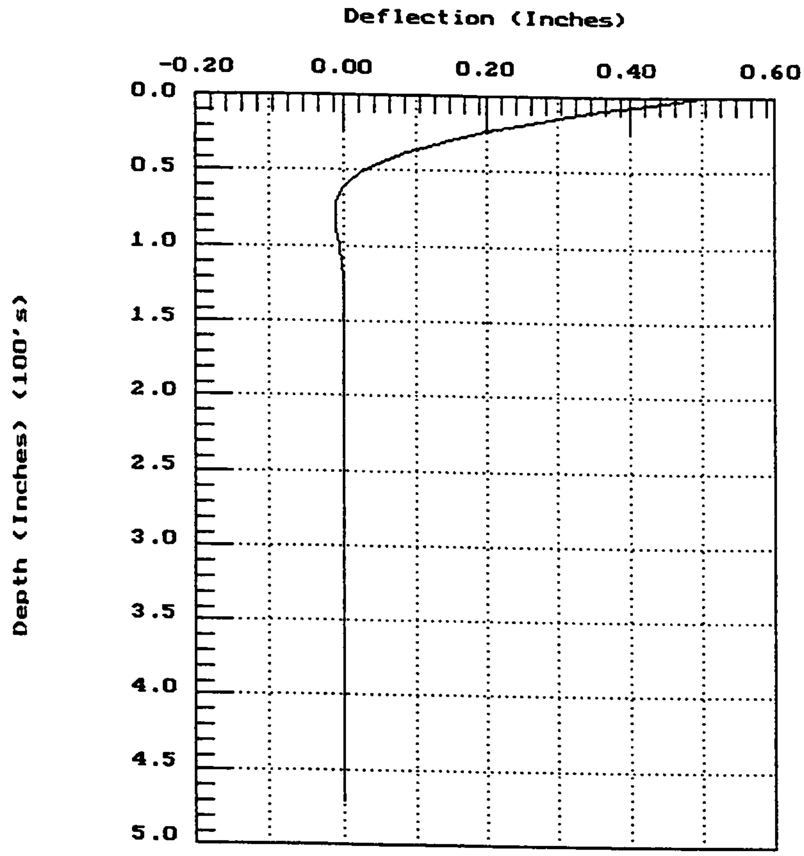

Deflection (Inches)
-0.20
0.00
0.20
0.40
0.60
0.0
0.5
1.0
1.5
2.0
2.5
3.0
3.5
4.0
4.5
5.0
Depth (Inches) (100's)

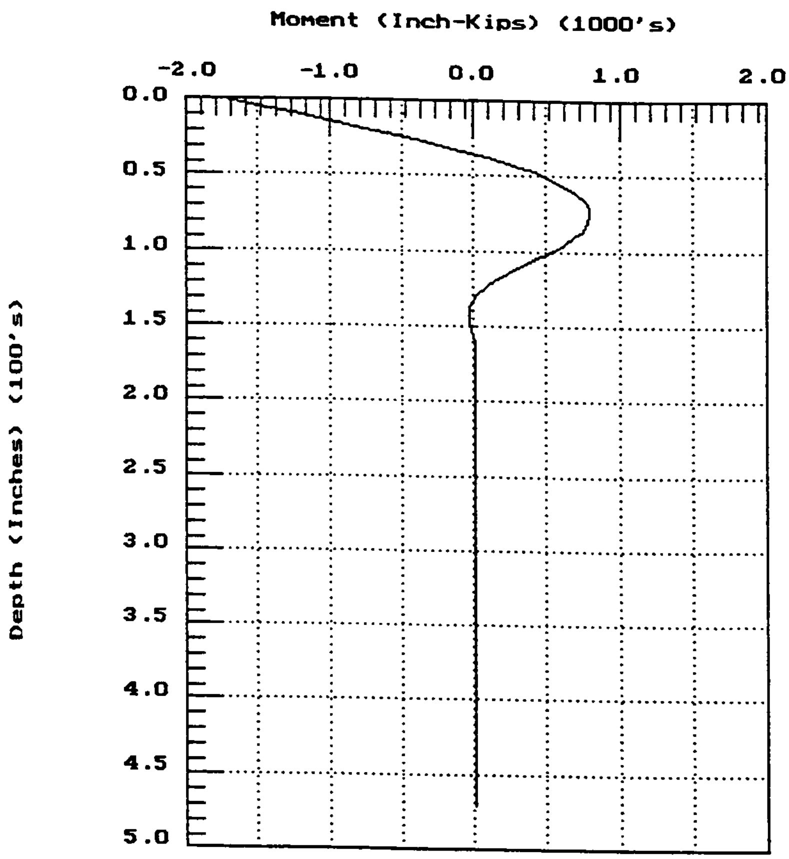
Moment (Inch-Kips) (1000's)
-2.0
-1.0
0.0
1.0
2.0
0.0
0.5
1.0
1.5
2.0
2.5
3.0
3.5
4.0
4.5
5.0
Depth (Inches) (100's)

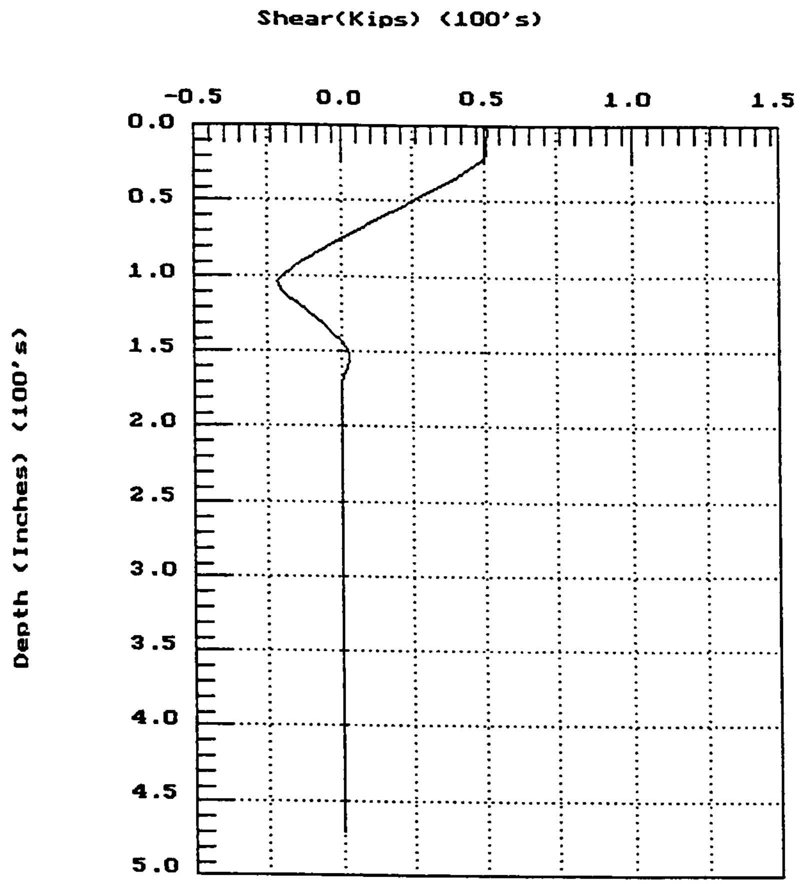

Shear(Kips) (100's)
-0.5
0.0
0.5
1.0
1.5
Depth (Inches) (100's)
0.0
0.5
1.0
1.5
2.0
2.5
3.0
3.5
4.0
4.5
5.0

Determination of additional shear required to
achieve 1" deflection.

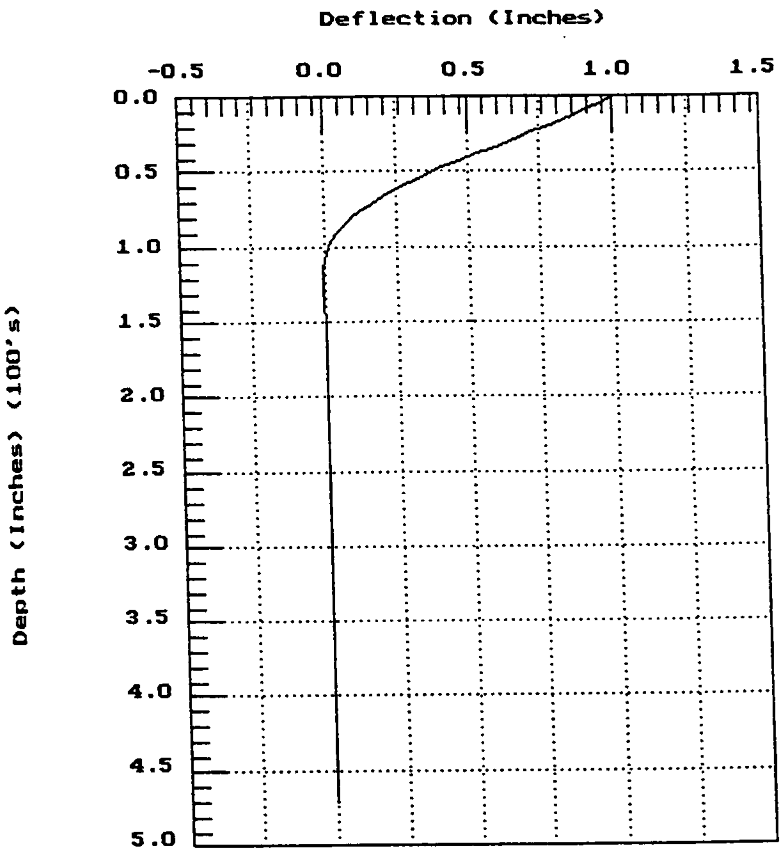

Deflection (Inches)
-0.5
0.0
0.5
1.0
1.5
0.0
0.5
1.0
1.5
2.0
2.5
3.0
3.5
4.0
4.5
5.0
Depth (Inches) (100's)

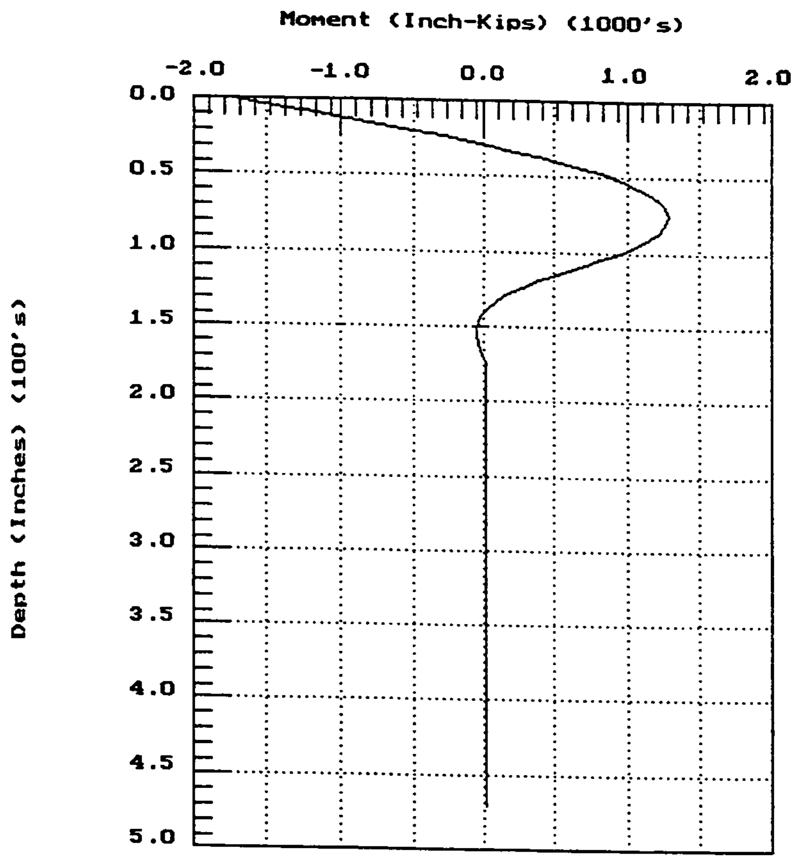

Moment (Inch-Kips) (1000's)
-2.0
-1.0
0.0
1.0
2.0
Depth (Inches) (100's)
0.0
0.5
1.0
1.5
2.0
2.5
3.0
3.5
4.0
4.5
5.0

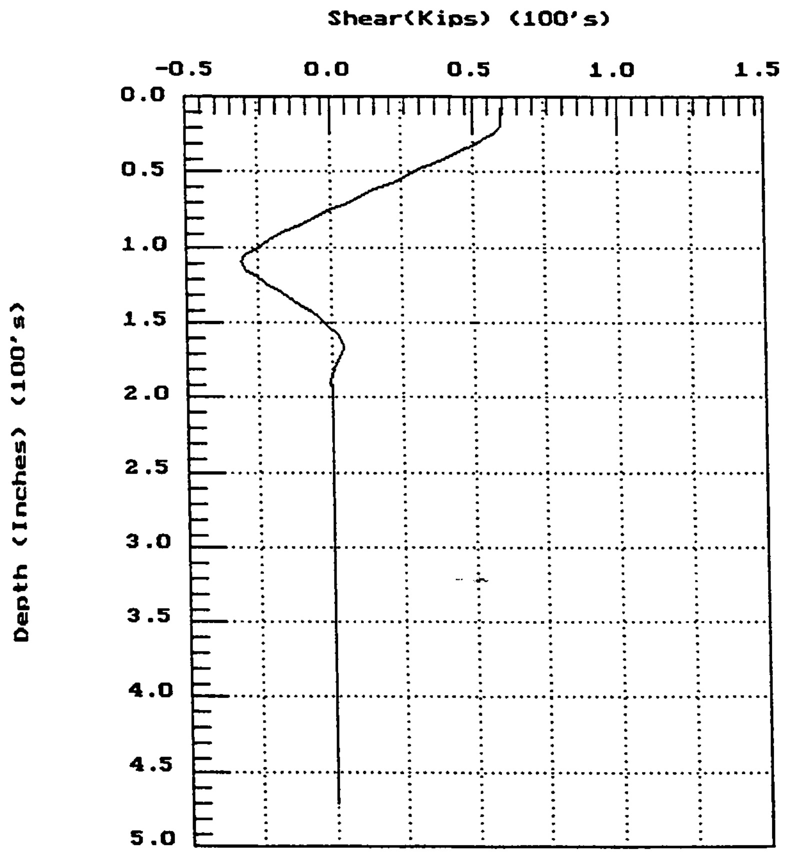
Shear(Kips) (100's)
-0.5
0.0
0.5
1.0
1.5
0.0
0.5
1.0
1.5
2.0
2.5
3.0
3.5
4.0
4.5
5.0
Depth (Inches) (100's)

APPENDIX D

CALCULATIONS

Determination of *a (in)* (Section 4.4)

Variables used in Equations

V *(kips)* -	50.3
M_{pile} *(kip-ft)* -	145
x *(in)* -	11

$$M_{pile} = 6.54R - 3.145V \qquad \text{(Eqn.4-3)}$$

R *(kips)* = 46.36

$$\sum Me = 0 = -6.54'R + \left(2.145' + \frac{12 - x}{2}\right) \cdot V + Fb(x) \qquad \text{(Eqn.4-4)}$$

Fb *(kips)* = 210.77

$$\sum Fx = 0 = V + Ft - Fb \qquad \text{(Eqn.4-2)}$$

Ft *(kips)* = 160.47

$$Fb = .85 \cdot f'c \cdot (a) \cdot (b) \qquad \text{(Eqn.4-1)}$$

a *(in)* = 2.48

new x *(in)* = 9.52

Determination of *a (in)* - continued

(Reiteration)

Variables used in Equations

V *(kips)* -	50.3
M_{pile} *(kip-ft)* -	145
x *(in)* -	9.09

$$M_{pile} = 6.54R - 3.145V \qquad \text{(Eqn.4-3)}$$

R *(kips)* = 46.36

$$\Sigma Me = 0 = -6.54'R + \left(2.145' + \frac{12 - x}{2}\right) \cdot V + Fb(x) \qquad \text{(Eqn.4-4)}$$

Fb *(kips)* = 249.77

$$\sum Fx = 0 = V + Ft - Fb \qquad \text{(Eqn.4-2)}$$

Ft *(kips)* = 199.47

$$Fb = .85 \cdot f'c \cdot (a) \cdot (b) \qquad \text{(Eqn.4-1)}$$

a *(in)* = 2.94

new x *(in)* = 9.06

Determination of *a (in)* (Section 4.4)

Variables used in Equations

V *(kips)* -	57.9
M_{pile} *(kip-ft)* -	145
x *(in)* -	11

$$M_{pile} = 6.54R - 3.145V \quad \text{(Eqn.4-3)}$$

R *(kips)* = 50.01

$$\sum Me = 0 = -6.54'R + \left(2.145' + \frac{12-x}{2}\right)\cdot V + Fb(x) \quad \text{(Eqn.4-4)}$$

Fb *(kips)* = 218.71

$$\sum Fx = 0 = V + Ft - Fb \quad \text{(Eqn.4-2)}$$

Ft *(kips)* = 160.81

$$Fb = .85 \cdot f'c \cdot (a) \cdot (b) \quad \text{(Eqn.4-1)}$$

a *(in)* = 2.57

new x *(in)* = 9.43

Determination of *a (in)* - continued

(Reiteration)

Variables used in Equations

V *(kips)* -	57.9
M_{pile} *(kip-ft)* -	145
x *(in)* -	8.95

$$M_{pile} = 6.54R - 3.145V \qquad \text{(Eqn.4-3)}$$

R *(kips)* = 50.01

$$\Sigma Me = 0 = -6.54'R + \left(2.145' + \frac{12-x}{2}\right)\cdot V + Fb(x) \qquad \text{(Eqn.4-4)}$$

Fb *(kips)* = 262.18

$$\sum Fx = 0 = V + Ft - Fb \qquad \text{(Eqn.4-2)}$$

Ft *(kips)* = 204.28

$$Fb = .85\cdot f'c\cdot(a)\cdot(b) \qquad \text{(Eqn.4-1)}$$

a *(in)* = 3.08

new x *(in)* = 8.92

Determination of Stress, *f (ksi)* (Section 4.4)

Variables used in Equations

V *(kips)* -	50.3
M_{pile} *(kip-ft)* -	145
x *(in)* -	9.06
a *(in)* -	2.94

$$M_{pile} = 6.54R - 2.145V \qquad \text{(Eqn.4-3)}$$

R *(kips)* = 46.36

$$\Sigma Me = 0 = -6.54'R + \left(2.145' + \frac{12 - x}{2}\right) \cdot V + Fb(x) \qquad \text{(Eqn.4-4)}$$

Fb *(kips)* = 250.51

$$Area_{In\ Shear} = (10" \cdot 20") + 2 \cdot (10" \cdot (a + 5"))$$

Area (in^2) = 358.80

$$\tau = \frac{F_b}{Area_{In\ Shear}}$$

τ (ksi)= 0.70

Determination of Stress, *f (ksi)* (Section 4.4)

Variables used in Equations

V *(kips)* -	57.9
M_{pile} *(kip-ft)* -	145
x *(in)* -	8.92
a *(in)* -	3.08

$$M_{pile} = 6.54R - 2.145V \qquad \text{(Eqn.4-3)}$$

R *(kips)* = 50.01

$$\Sigma Me = 0 = -6.54'R + \left(2.145' + \frac{12 - x}{2}\right) \cdot V + Fb(x) \qquad \text{(Eqn.4-4)}$$

Fb *(kips)* = 262.96

$$Area_{In\ Shear} = (10"\cdot 20") + 2\cdot(10"\cdot(a + 5"))$$

$Area$ (in^2) = 361.60

$$\tau = \frac{F_b}{Area_{In\ Shear}}$$

τ (ksi)= 0.73

VITA

Kenneth Ryan Harvey was born in Lenoir City, Tennessee on September 13, 1972. In May, 1990 he graduated from Lenoir City High School and enrolled at The University of Tennessee. He received a Bachelor of Science degree in Civil Engineering from The University of Tennessee in December, 1995. He began graduate school in the Spring of 1996 and received his Master of Science degree in Civil Engineering in May, 1997.